Palaeogeography, Palaeoclimatology, Palaeoecology 399 (2014) 294–309

Contents lists available at ScienceDirect

Palaeogeography, Palaeoclimatology, Palaeoecology

journal homepage: www.elsevier.com/locate/palaeo

Integrated reconstruction of Holocene millennial-scale environmental changes in Tierra del Fuego, southernmost South America ☆

Nicolás Waldmann [a,*], Ana Maria Borromei [b], Cristina Recasens [c,d], Daniela Olivera [b], Marcelo A. Martínez [b], Nora I. Maidana [e], Daniel Ariztegui [c], James A. Austin Jr. [f], Flavio S. Anselmetti [g], Christopher M. Moy [h]

[a] Dr. Moses Strauss Department of Marine Geosciences, Charney School of Marine Sciences, University of Haifa, Mount Carmel, 31905 Haifa, Israel
[b] INGEOSUR, CONICET, Departamento de Geología, Universidad Nacional del Sur, B8000ICN Bahía Blanca, Argentina
[c] Section of Earth & Environmental Sciences, University of Geneva, 1205 Geneva, Switzerland
[d] Lamont-Doherty Earth Observatory, Columbia University, Palisades, New York 10964, NY, USA
[e] Departamento de Biodiversidad y Biología Experimental, Facultad de Ciencias Exactas y Naturales, Universidad de Buenos Aires, C1428EHA Buenos Aires, Argentina
[f] Institute for Geophysics, John A. and Katherine G. Jackson School of Geosciences, University of Texas at Austin, TX 78758, USA
[g] Institute of Geological Sciences and Oeschger Centre for Climate Change Research, University of Bern, 3012 Bern, Switzerland
[h] Geology Department, University of Otago, 9054 Otago, New Zealand

ARTICLE INFO

Article history:
Received 8 August 2013
Received in revised form 22 January 2014
Accepted 26 January 2014
Available online 1 February 2014

Keywords:
Lacustrine sediments
Paleoenvironment and Paleoclimate reconstruction
Palynology
Limnogeology
Southern Hemisphere Westerlies
Multi-proxy analyses

ABSTRACT

This study presents new paleoenvironmental data obtained from sedimentary cores from Lago Fagnano, an elongated lake located at 54°S in southernmost South America. Data from palynomorphs (pollen, spores and algae) and associated palynofacies as well as from diatom taxa retrieved from these cores compared with other regional proxies contribute to evaluate the similarities and differences in the climate patterns based on different proxies from southernmost Patagonia. The pollen analysis reveals that a grass steppe environment existed during the early Holocene (11,300–~8000 cal a BP) followed by a major vegetation change characterized by development of forest-steppe ecotone communities between ~8000 and ~6500 cal a BP, under more humid conditions. Between ~6500 and ~4000 cal a BP, expansion and colonization by *Nothofagus* forests reflect an increase in effective moisture levels, while openness in the forest communities characterizes the region after ~1100 cal a BP. The palynological organic matter combined with the algal content reflects hydrological changes occurring in the lake and its nutrient status, probably in close relation with past climate oscillations. All these past ecological changes are closely related to oscillations in precipitation and temperature as a response to the variations in the latitudinal position and/or strength of the Southern Westerlies wind belt during the Holocene.

1. Introduction

Comprehensive high-resolution multi-proxy studies of Holocene environmental changes in continental sedimentary archives from Tierra del Fuego (southernmost South America) are scarce and limited in space and time. Furthermore, the region is currently directly situated in the path of the Southern Hemisphere Westerlies wind stream (SHW) and only ~5° north of the Antarctic Frontal Zone (AFZ). This climatic situation has considerably changed during the past glacial–interglacial cycles. Tierra del Fuego is thus well located to address questions related to timing and amplitudes of Holocene climate fluctuations and to assess the impact of such variations in the long-term biomass in this region.

Most paleoenvironmental reconstructions from Isla Grande de Tierra del Fuego have been carried out along the Beagle Channel (Auer, 1960; Heusser and Rabassa, 1987; Heusser, 1989, 1998; Pendall et al., 2001; Grill et al., 2002; Heusser, 2003; Borromei and Quattrocchio, 2008; Candel et al., 2009; Markgraf and Huber, 2010), on the low inner valleys of the Fuegian Andes (Borromei, 1995; Borromei et al., 2007a, 2007b) and within several hanging Andean valleys (Markgraf, 1993; Borromei et al., 2010; Markgraf and Huber, 2010) (Fig. 1A and B). Yet, studies completed on the northern and central parts of the archipelago are still scarce (Markgraf, 1980; Heusser, 1993; Heusser and Rabassa, 1995; Burry et al., 2006). The current contribution presents palynomorph analysis (pollen, spores and algae) and associated palynofacies, combined with additional identification of diatom flora obtained from sedimentary cores retrieved at different locations and water depths from Lago Fagnano (Fig. 1C). The current study complements existing published information on geochemical (Waldmann et al., 2010a) and bulk C and N stable isotope studies (Moy et al., 2011) that were carried out in these cores. Thus, the new combined dataset allows reconstructions of the mechanisms controlling millennial-scale Holocene environmental changes in Tierra del Fuego.

☆ All the authors equally contributed to this manuscript.

* Corresponding author. Tel.: +972 4 8280736.
E-mail address: nwaldmann@univ.haifa.ac.il (N. Waldmann).

0031-0182/$ – see front matter © 2014 Elsevier B.V. All rights reserved.
http://dx.doi.org/10.1016/j.palaeo.2014.01.023

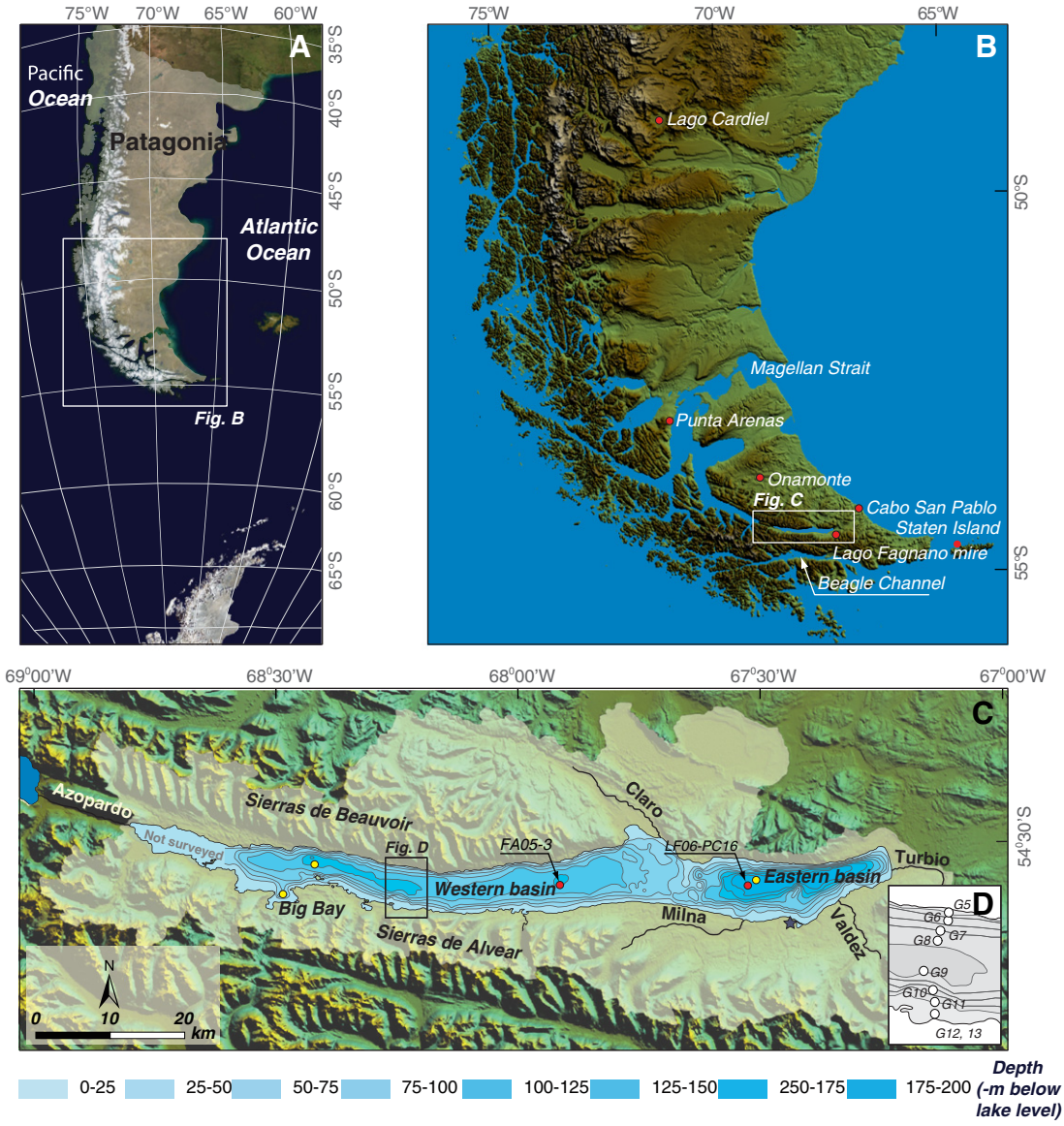

Fig. 1. A) Satellite image of southernmost South America. The light shading highlights Patagonia, while the white rectangle marks the location of insert B. B) Southernmost Patagonia and the Tierra del Fuego archipelago with the locations of the main sites discussed in this paper marked with red dots. The rectangle notes the location of C. C) Lago Fagnano watershed (light-shaded area) with the main fluvial systems. The bathymetry of Lago Fagnano is shown with a contour interval of 25 m (following Waldmann et al., 2010a). The location of sedimentary cores FA05-3 and LF06-PC16 (red circles), the water column measurements (yellow circles) and the meteorological station (gray star) are shown as well. Distance between the two cores is ~25 km. The rectangle stands for the location of D. D) Enlargement of the western sub-basin area with the location of the surface sediment grab samples (white circles) used for modern diatom identification and other surface sediment analyses.

2. Regional setting

2.1. Geology and geomorphology

The archipelago of Tierra del Fuego is located at the southernmost extreme of Patagonia, only ~1000 km north of the Antarctic Peninsula (Fig. 1A). The study site Lago Fagnano (named Kami in the native Selk'nam language) is located in the central part of the main island (~54°S). This E–W elongated lake (~105 km length and ~10 km width) occupies a total area of ~560 km^2, has a water level of only ~26 m above mean sea level (amsl) and is the largest ice-free water body in the high southern latitudes outside Antarctica. Lago Fagnano comprises two sub-basins: a smaller, deeper sub-basin in the east, reaching a maximum depth of ~210 m, and a western elongated and shallower sub-basin of ~110 m water depth (Fig. 1C).

The Fagnano basin is the deepest continental pull-apart structure in a series of graben-shaped, asymmetric tectonic sinks organized in an *en-échelon* arrangement along the Magellan–Fagnano Transform system (MFT), which separates the Scotia and South American plates (Menichetti et al., 2008, and references therein). The basin was further deepened during past glaciations, when ice streams originating from the Darwin Cordillera expanded eastwards through the tectonic basin, leaving behind a series of terminal moraines. While some of these moraine morphologies are partially exposed in the lake surroundings (Coronato et al., 2009), most are covered by thick lacustrine sedimentary units and can only be identified under the lake's subsurface (Waldmann et al., 2010b). Thus, the origin and evolution of this lake basin lies in a combination of glacial and tectonic processes, as this basin developed in a tectonic setting repeatedly carved by glacial activity (Waldmann et al., 2008).

2.2. Lago Fagnano hydrology and limnology

Relatively little is known about the modern limnology and limnic ecosystem of Lago Fagnano. Recent studies show that although lake-level oscillations of Lago Fagnano are minor and in the scale of less than a meter, they cannot be neglected since they show a pronounced seasonal cycle (Richter et al., 2010). Previously collected surface water samples indicate an ultra-oligotrophic to oligotrophic lake, with high water transparency and reduced algal biomass representing a lacustrine environment typified by very low nutrient content (Table 1) (Mariazzi et al., 1987; Quirós et al., 1988; Quirós and Drago, 1999). Several perennial streams feed the lake, such as the Claro, Milna, Valdez and Turbio, which are the principal rivers flowing into this lake. Only one fluvial outlet, the Azopardo, drains the lake at its westernmost extreme into the Almirantazgo Fjord (Admiralty Sound) towards the Strait of Magellan (Fig. 1C).

2.3. Climate and vegetation

Tierra del Fuego's climate is sub-polar, characterized by cold and relative dry winters and mild but windy short summers. Precipitation increases during summer seasons with the influence of the SHW. A meteorological station installed in 2004 on the southern shore of the lake (see Fig. 1C for location) served as the main source of data used in this study (Fig. 2). Measurements taken between 2004 and 2008 clearly show the dominating influence of the SHW (Fig. 2B and C). This wind belt migrates southwards during austral summers (Lamy et al., 2002; Moy et al., 2009; Moreno et al., 2010; Björck et al., 2012), bringing moisture and humidity to the region. This moisture originates from the Pacific Ocean and is related to the subtropical anticyclone in the Southeast Pacific and the circum-Antarctic low-pressure belt (Rogers and van Loon, 1982). Austral winters however, are mostly influenced by Antarctic Oscillation (AAO), promoting drier but colder conditions (Montgomery et al., 2001). These large-scale ocean–atmosphere interactions play a key-role in modifying not only the precipitation amount and its distribution through changes in the strength and latitudinal position of the SHW, but also in influencing temperatures at seasonal to inter-annual timescales (Garreaud et al., 2009).

Modern vegetation in the island of Tierra del Fuego is characterized by the Fuegian–Patagonian steppe in the north, where mean annual precipitation is <400 mm, gradually changing southward to the Subantarctic Deciduous and Evergreen Forest, which characterizes areas with increased precipitation and high topographic gradients (Fig. 3). These southern forests include three species of southern beech: *Nothofagus pumilio*, *N. betuloides* and *N. antarctica*, which all grow from sea level to an average altitude of 550–600 m amsl. Deciduous forests predominate where precipitation averages between 400 and 800 mm/yr, and evergreen forests occur to the west and south along the Beagle Channel, coincident with the outer zone of the heavy precipitation, >800 mm/yr (Heusser, 1998). Magellanic moorland occurs beyond the forest boundaries along the exposed south and westernmost coasts under increased precipitation conditions, >1000 mm/yr, accompanied by high winds and poor drainage. High-Andean desert vegetation typically develops at high-altitude areas in the Fuegian cordillera above the tree line, >600 m amsl (Heusser, 2003).

Table 1
Surface water characteristics of Lago Fagnano measured in summer 1986, spring 1984, and spring 2002 (Mariazzi et al., 1987; Quirós et al., 1988). TP: total phosphorous concentrations, TN: total nitrogen concentrations, Chl: concentrations of chlorophyll type a, SDL: water transparency.

	TP (mg/m^3)	TN (mg/m^3)	Chl (mg/m^3)	SDL (m)
Summer 1986	2	410	0.49	11.5
Spring 1984	12	na	0.27	9
Spring 2002	7	163	na	na

3. Materials and methods

3.1. Water sampling and vertical profiling

During the November 2006 field season, the water column was sampled at three locations with a Niskin bottle (Fig. 1C for sample locations). Dissolved oxygen (mg/l), temperature (°C) and pH were measured on site at 5–20 m depth-intervals according to the weather conditions. The water samples were sealed and stored under dark conditions on land at 4 °C prior to transport for further chemical analyses.

3.2. Coring and associated geochemical analysis

A total of 18 cores were retrieved during the two field seasons (2005–2006), including 5 short gravity cores of ~2.20 m maximum length and 13 Kullenberg-type piston cores of up to 8.50 m in length. Coring sites were targeted at selected locations based on previously acquired and interpreted seismic data (Waldmann et al., 2008). This paper concentrates on data retrieved from piston core LF06-PC16 and gravity core FA05-3, that together represent the sedimentation pattern in both the eastern and western sub-basins of the lake, respectively (see Fig. 1C for core locations). Core LF06-PC16 was retrieved at a water depth of 196 m and measures ~7.30 m and core FA05-3, retrieved at 127 m water depth is 1.60 m long and has a well-preserved sediment–water interface. Amalgamating the new pollen and diatom data presented in this paper with previously published geochemical information from the same cores, provides a complete set of proxies that allows a better comprehension of paleoenvironmental changes of the region.

After their retrieval, the cores were cut into 1 to 1.5 m pieces for transport and further stored in a dark cold room at 4 °C at the laboratory facilities in the University of Geneva. The cores were subsequently scanned at the ETH-Zurich with a GEOTEK™ multi-sensor core logger (MSCL) to obtain the petrophysical properties of the sediments in a non-destructive fashion (P-wave velocity, gamma-ray attenuation bulk density and magnetic susceptibility). The sediment cores were photographed immediately after splitting and their sedimentary record was described in detail prior to possible deterioration due to oxygen exposure. Preliminary sampling included smear-slide analysis to characterize sediment components. Elemental chemistry at ~50 μm resolution was measured at the University of Geneva with a non-destructive Röntgenanalytik Eagle II micro X-Ray Fluorescence (XRF) system. Acquisition parameters of the Rh tube were set at 40 kV and 800 mA. Furthermore, the percentage of total organic carbon (TOC) was measured in dried powdered samples with a Rock-Eval (Re6) analyzer at the University of Neuchâtel, for constraining the amount of total organic and inorganic carbon in the sediments.

3.3. Chronological analysis

The chronology for the present study is based on previous works by Moy et al. (2011) and Waldmann et al. (2011) (Table 2). Terrestrial organic material retrieved at different depths of the cores served for further AMS ^{14}C analysis (for detail on radiocarbon methodology, see Bertrand et al., 2012). Radiocarbon dates were converted to calendar years before present (cal yr BP) using the CALIB 6.0 program (Stuiver et al., 2005). Potential contamination by old or "dead" carbon sources within the watershed and/or by remobilization and deposition of older sediments is possible, so we treated these ages as maximum values for their corresponding stratigraphic levels. Yet, the presence of a tephra layer in the sedimentary record geochemically fingerprinted to the Hudson H1 ash (Waldmann et al., 2010a), dated to 7570 + 110/−140 cal a BP (Naranjo and Stern, 1998; Stern, 2008) provides the extraordinary advantage to corroborate radiocarbon data. A previous

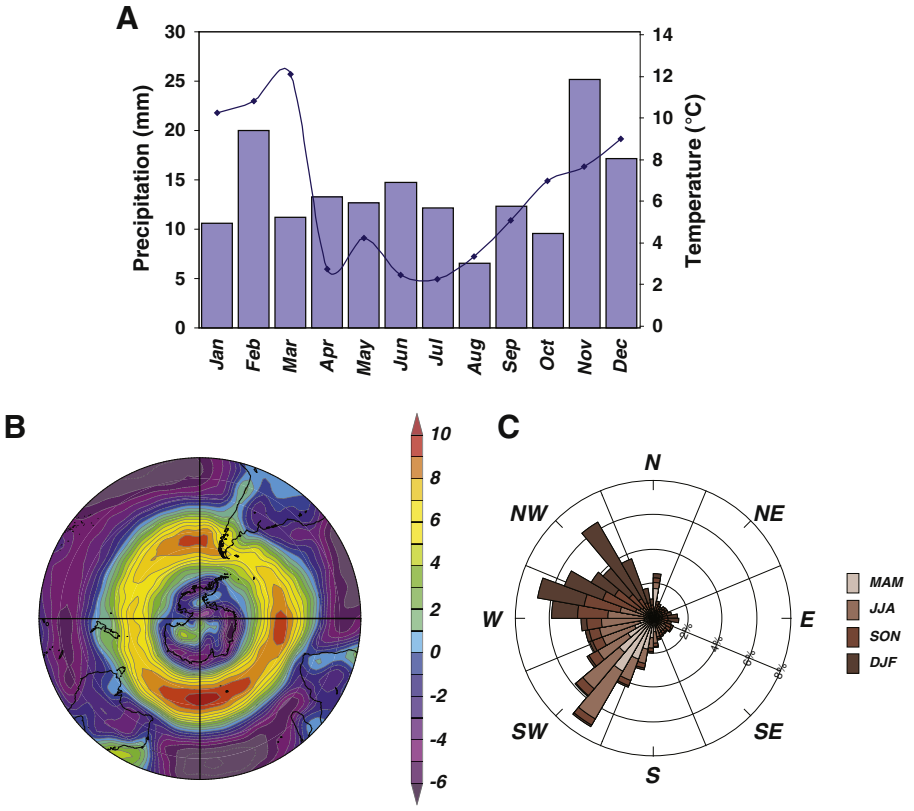

Fig. 2. A) Mean monthly precipitation (blue bars) and mean monthly temperature (blue dots) for the 2004–2008 time period at the meteorological station located on the southern shores of Lago Fagnano (see Fig. 1C). B) 1000 mb zonal winds during the austral summer over the southern hemisphere, calculated for the 1972 to 2005 time period (Kalnay et al., 1996). Regional precipitation measurements are directly connected to the Southern Hemisphere Westerlies. Note the increasing values of zonal winds over Tierra del Fuego. C) The relative frequency (%) of the annual distribution of the wind direction (2004–2008), as recorded by a meteorological station located on the southern shores of Lago Fagnano (see Fig. 1C). The different color bars stand for different seasons (MAM: March, April and May; JJA: June, July and August; SON: September, October and November and DJF: December, January and February).

study using core LF06-PC16 (Waldmann et al., 2010a), complemented with further radiocarbon dating of pollen concentrates by Moy et al. (2011), shows that both radiocarbon and tephra data are robust for estimating sedimentation rates. We have been able to develop a consistent age model that allows us to assign interpolated calendar ages to the different sampled depths of core LF06-PC16 (Table 3), thereby overcoming the obstacles mentioned above to construct a reliable sediment–core chronology.

3.4. Palynomorph and palynofacies analyses

Samples for palynological analysis extracted from core LF06-PC16 were processed according to standard techniques (Faegri and Iversen, 1989). *Lycopodium* spore tablets added to each sample prior to treatment (Stockmarr, 1971) allowed calculation of palynomorph concentration per gram of dry weight of sediment. Frequencies (%) of tree, shrub and herb pollen were calculated from sums mostly of >150 grains, while frequencies (%) of cryptogam spores and algae (*Botryococcus braunii* and *Pediastrum kawraiskyi*) were calculated separately and related to the basic pollen sum. Change stratigraphically constrained cluster analysis to constrained incremental sum of squares cluster analysis (CONISS; Grimm, 1987) was applied to distinguish pollen zones based on taxa that reached >1% of the basic pollen sum.

Samples for palynofacial analysis were mounted using a glycerine-based jelly, after chemical removal (HCl and HF) of the mineral matrix and sieving through a 10 μm mesh screen. The palynological matter was systematically examined under normal transmitted light. The palynofacies analysis was carried out following the methods described by Tyson (1995) and Batten (1996), distinguishing four categories of palynological matter (PM), comprising 1) structured, translucent and opaque phytoclasts, 2) amorphous organic matter (AOM), 3) palynomorphs (pollen, spores and algae) and 4) zooclasts. The relative percentage of sedimentary organic constituents was based on counting at least 500 particles per sample. The palynofacies totals were then grouped into different palynofacies types, based on the occurrence of relative frequencies of the four palynomorph categories. For this purpose, a cluster analysis from Paleontological Statistics was performed (PAST; Hammer et al., 2001).

3.5. Diatom flora analysis

Determination of modern diatom flora and their spatial distribution within the lake was accomplished using surface-sediment samples taken along a N–S transect crossing the lake from shallow- to deep-water environments (Fig. 1C for sampling sites). Core FA05-3 was used for determining the temporal distribution of the diatom assemblages and the relative abundances of the different species. The laminated section of the core (uppermost 1.20 m) was sampled (~1 mg) every 10 laminae couplets. Sample treatment and slide mounting were carried out at the Geomicrobiology Laboratory facilities at the University of Geneva following standard procedures further described by Battarbee (1984, 1986). Sample treatment consisted of sediment digestion in 30% hydrogen peroxide at room temperature followed by warming in a hot bath to accelerate the remaining reaction until fizzing stopped (not all digestion was done in the hot bath due to extreme reactivity of the solution). A few drops of 10% HCl were added to totally stop the reaction and remove all carbonate content. The samples were rinsed several times with deionized water to re-equilibrate their pH and a few drops of 20% NH_3 were added in the last rinse to slow clay decantation and facilitate its removal. Samples were then mounted onto

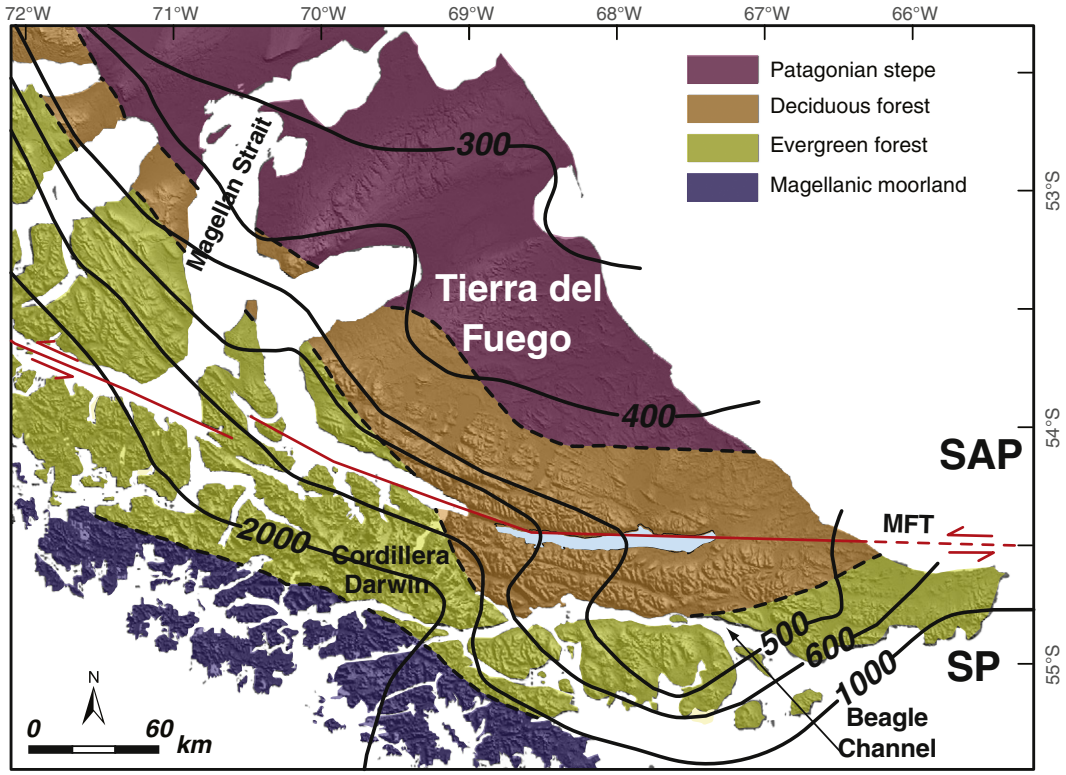

Fig. 3. High-resolution digital elevation model (Mercator projection) from processed Shuttle Radar Topography Mission data (SRTM; Farr et al., 2007) from NASA of the Isla Grande de Tierra del Fuego. The distribution of major vegetation units (colored areas) and precipitation gradients (continuous contours) are marked on top of the SRTM map (from Moreno et al., 2009). The main tectonic features: MFT: Magallanes–Fagnano Transform fault system, SAP: South American Plate, SP: Scotia Plate.

microscope slides with Naphrax following standard procedures for further quantitative and qualitative analyses (Battarbee, 1986). In order to calculate relative frequencies, a minimum of 1500 valves was counted per slide using a phase contrast Leitz Diaplan light microscope at X1000 magnification under oil immersion. Diatom profiles were plotted using the software C2 (Juggins, 2003) and diatom zones were determined based on a CONISS cluster analysis (Stratigraphically Constrained Incremental Sum of Squares; Grimm, 1987) using the computer program TILIA and TGView 2.0.2; (Grimm, 1993, 2004).

4. Results

4.1. Modern limnology

Three water column profiles were measured in this study (November 2006) at different locations and water depths across the lake: the western basin, the eastern basin and the Big Bay site (see Fig. 1C for locations). The water profiles are characterized by small vertical changes in pH, temperature, and oxygen content (Fig. 4). The Big Bay profile, however,

Table 2
Summary of radiocarbon dates used in this study and obtained from different cores in Lago Fagnano bulk sediments, pollen concentrates and terrestrial macrofossils (Moy et al., 2011; Waldmann et al., 2011).

Number	Sample ID	Core	Core depth (cm)	Modified depth without turbidites	Material	Age	Error	Median probability age (cal yr BP)	2σ lower	2σ upper
1	115796	LF01	0	0	Bulk organic	6150	30	6960	160	190
2	115797	LF01	45	27	Bulk organic	5720	35	6450	130	110
3	115798	LF01	74	51	Bulk organic	6740	35	7550	80	70
4	115799	LF01	112	85	Bulk organic	9235	35	10,340	100	150
5	115800	LF01	157	130	Bulk organic	11,125	35	13,030	90	80
6	118297	LF01	25	11	Pollen-1.6 g/cm3	1015	35	860	70	90
7	118298	LF01	52	34	Pollen-1.6 g/cm3	1920	30	1800	90	80
8	118366	LF01	52	34	Pollen-1.6 g/cm3	1680	70	1520	150	180
9	118364	LF01	73	50	Pollen-1.6 g/cm3	2565	35	3590	130	160
10	118365	LF01	111	84	Pollen-1.6 g/cm3	4495	50	5060	190	230
11	118366	LF01	158	129	Pollen-1.6 g/cm3	5335	50	6070	140	130
12	118367	LF01	111	84	Terrestrial macro	3410	50	3590	140	130
13	128995	PC18	10	-	Terrestrial macro	505	35	510	20	30
14	128996	PC18	61.5	-	Terrestrial macro	2610	35	2630	140	130
15	-	PC18	240	170	Mean pooled age	6850	10	7660	240	300
16	-	PC16	612	750	Terrestrial macro	10,435	75	12,360	190	180
17	-	PC16	318	390	Terrestrial macro	5445	125	6210	150	160

Table 3
Calculated calibrated ages of selected samples from core LF06-PC16, which serve to construct a representative age-depth model (see details in the text). The overall sedimentation rate is calculated to be 0.54 mm/y (from Waldmann et al., 2010a). Tephra age is marked in italics.

Depth (cm)[a]	*Calculated (yr BP)*[b]
10	56
40	574
80	1110
120	1815
170	2700
190	2980
250	4050
262	4145
330	5240
390	6090
442	6980
460	7110
490	7570
520	8070
535	8270
600	9290
620	9620
670	10,140
695	10,490
748	11,300

Sedimentation rate: 0.54 mm/yr.

exhibits some significant variations in the measured parameters, mainly in the oxygen content, which varies from 6 mg/l at the surface to 12 mg/l at 30 m water depth and back to ~7 mg/l at 70 m, close to the Bay's deepest level. We suggest that the oxygen content profile at the Big Bay site may be associated with deep-water circulation across the sill that divides the Big Bay sub-basin from the deeper, western sub-basin. In all water profiles, no significant thermocline is detected, suggesting a well-mixed lake when the profiles were collected. However, during the November 2006 field season, the lake level was ~1.5 m higher than normal due to extreme precipitation. We estimate that the higher-lake-level conditions caused flooding and erosion of coastal areas, increasing detrital material concentration in the water column across the lake, possibly favoring vertical mixing.

4.2. Sedimentology and petrophysics

4.2.1. Piston core LF06-PC16

Previous studies showed the presence of two lithological units: E1 (bottom) and E2 (top) that are mainly distinguished by slight color changes (Waldmann et al., 2010a). Unit E1 (~70 cm) consists of alternating pale-brown, silty clay to clay-sized mud with 0.5–1.0 cm-thick laminations, while unit E2 (66x-0 cm) consists entirely of brown 0.5–1.0 cm-thick silty clay laminae with thinner, 0.5–2.0 mm-thick, dark-green to black, clay-enriched laminae. E2 is frequently interrupted by 3 to 15 cm-thick, light brown, graded layers composed of fine sand, silt and clay with relatively high magnetic-susceptibility values interpreted as turbidites (Waldmann et al., 2011). Petrophysical parameters (i.e., magnetic susceptibility and density) usually increase at these interpreted turbiditic levels, supporting an allochthonous origin.

Overall bulk density and magnetic-susceptibility values increase proportionally down-core (Fig. 5). Very high magnetic-susceptibility values at 4.80 m depth correspond to the Hudson H1 ash identified in this core (Waldmann et al., 2010a). The H1 tephra served as a chronological marker as well as for stratigraphical correlation between the different cores.

4.2.2. Gravity core FA05-3

Core FA05-3 only recovered lithostratigraphic unit W4 (Waldmann et al., 2010a. This lithostratigraphic unit consists of fine alternations (<2 mm) of black and brownish laminae, in a similar fashion as unit E2. In comparison with unit E2 from the eastern sub-basin, the sedimentary succession is here continuous and only interrupted once by a slightly graded thin layer (3 cm) of very fine silt to clay interpreted as a turbiditic event (Waldmann et al., 2011). A tephra, identified as the

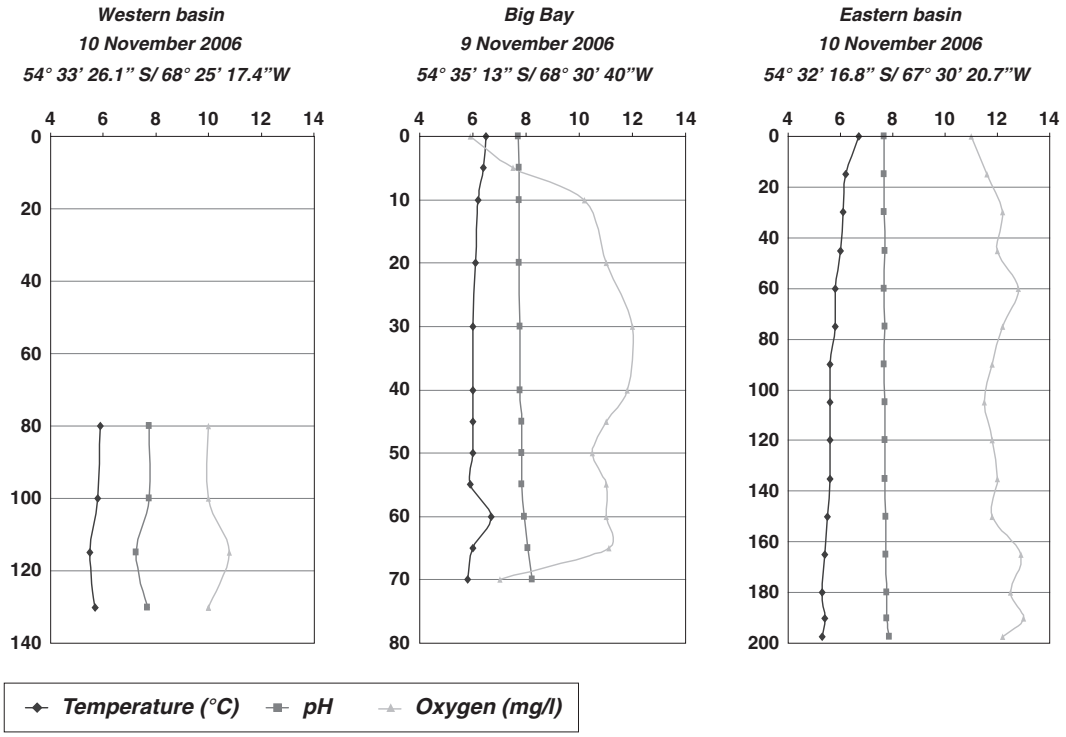

Fig. 4. Vertical water profiles in the western basin, the Big Bay site and the eastern basin of Lago Fagnano (see Fig. 1 for location). Note the vertical variation in scale between the profiles. The western basin site was not sampled above 80 m water depth as a consequence of weather conditions. For location of the different profiles, see Fig. 1C.

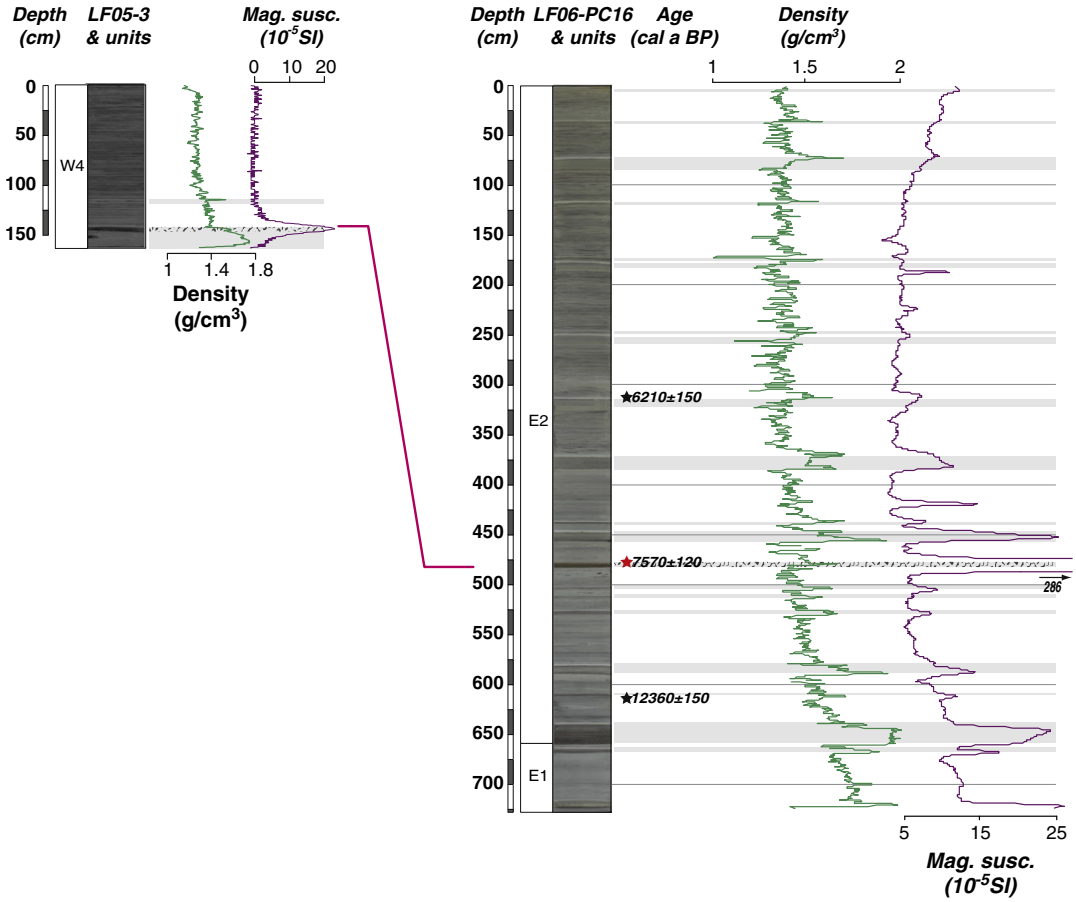

Fig. 5. Core photographs and petrophysical data (bulk density and magnetic susceptibility) for gravity core FA05-3 (left) and LF06-PC16 (right). Shaded horizontal bars stand for identified turbidites. Red star mark the H1 Hudson tephra age and black stars stand for radiocarbon ages. Red line marks the level H1 Hudson tephra identified in both cores serving for chronological marker and correlation among cores. See text for further details.

H1 event, was retrieved at a depth of 1.4 m. This ash layer overlies a massive turbidite layer of over 10 cm.

In general, bulk density slightly increases down-core (from 1.2 to 1.4 g/cm^3) while the magnetic susceptibility remains stable at ~ zero values throughout the entire recovered laminated sequence. Further below at 1.50 m at the H1 tephra layer, bulk density and magnetic susceptibility greatly increase to 1.6 g/cm^3 and 22 × 10^{-5} SI, respectively. In the basal turbidite layer, bulk density increases to 1.8 g/cm^3 while the magnetic-susceptibility values decrease to almost zero.

4.3. Palynomorph analysis

The pollen record was only retrieved from core LF06-PC16 since it covers a longer time interval. It was divided into three zones and subsequent subzones on the basis of cluster analysis and visual inspections (zones LF-1, LF-2 and LF-3, respectively; Fig. 6).

The evergreen tree species *N. betuloides* and the deciduous tree species *N. pumilio* and *N. antarctica* are shown collectively as "*Nothofagus dombeyi* type", given the difficulty in species separation. The fossil pollen spectra were compared with regional pollen spectra from surface-soil samples (Heusser, 1989; Musotto et al., 2012) and with present-day vegetation from Tierra del Fuego (Pisano, 1977; Heusser, 2003).

4.3.1. Zone LF-1 (730–500 cm depth, ~11,300–~8000 cal a BP)

4.3.1.1 . Pollen. This zone is characterized by low pollen content at 5.17, 6.02 and 6.91 m depth (samples 44, 51 and 57). At 5.76 and 7.27 m depth, the samples only record traces of pollen taxa (samples 49 and 60). At 6.61 m depth (sample 54), the pollen assemblage is dominated by Poaceae (48%), *Empetrum*/Ericaceae (13%) and Pteridophyta (15%), accompanied by Asteraceae subf. Asteroideae (6%) and Cyperaceae (7%). Other herbaceous taxa (Caryophyllaceae, *Gunnera*, Apiaceae, *Acaena*, *Gentiana*, Asteraceae subf. Cichorioideae, Chenopodiaceae and *Myriophyllum*) are present in low frequencies (<3%). Frequencies of *Nothofagus dombeyi* type are minimal (12%). Overall, very low total pollen concentration values are observed in this zone (1400 grains/g).

4.3.1.2. Algae. At 6.61 m depth (sample 54), *Botryococcus braunii* (Fig. 7A to D) amounts to 12%, *Pediastrum kawraiskyi* (Fig. 7E to H) 2.5% and *Zygnema*-type <2%.

4.3.2. Zone LF-2 (500–250 cm depth, ~8000–~4000 cal a BP)

4.3.2.1. Pollen. Two subzones can be differentiated based on proportional changes of non-arboreal and arboreal taxa. Subzone LF-2a (8000–~6500 cal a BP) displays an increase in *Nothofagus dombeyi* type (26%) frequencies, accompanied by Poaceae (36%), *Empetrum*/Ericaceae (12%), Asteraceae subf. Asteroideae (11%), and Chenopodiaceae (9%) along with Cyperaceae (12%). Other herbaceous taxa, like Caryophyllaceae, *Gunnera*, Apiaceae, *Acaena*, *Gentiana*, Asteraceae subf. Cichorioideae and Brassicaceae are also present in low quantities (<4%). *Misodendrum*, mistletoe on *Nothofagus*, also appears in low quantities but becomes continuous. Subzone LF-2b (~6500–4000 cal a BP) shows an increase in *Nothofagus dombeyi* type values, from 37 to 62%, and a decline in Poaceae from 27 to 11%. Shrubs (*Empetrum*/Ericaceae and Asteraceae subf. Asteroideae) and herbs (Chenopodiaceae) as well as aquatic taxa (Cyperaceae) decline upward in the core (<9%). The total pollen concentration

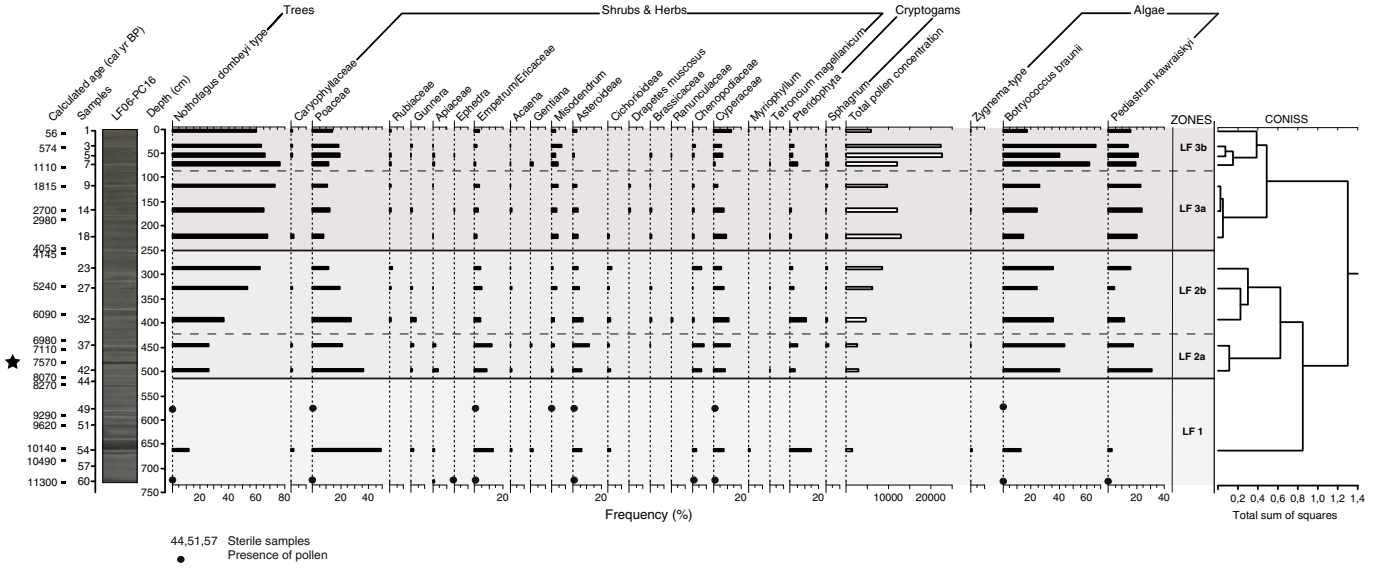

Fig. 6. Frequencies (%) of pollen, algae and total pollen concentrations (grains/g) obtained from core LF06-PC16. Frequencies of algae (*Botroyococcus braunii* and *Pediastrum kawraiskyi*) are shown in relation to terrestrial pollen.

values increase upcore from 2700 grains/g (subzone LF-2a) to 8400 grains/g (subzone LF-2b).

4.3.2.2. Algae. Botryococcus braunii occurs at high values, varying between 24 and 43%, while *Pediastrum kawraiskyi* shows lower values (18–31%) in subzone LF-2a, overlain by an abrupt decline (11–16%), reaching minimum values (5%) within subzone LF-2b.

4.3.3. Zone LF-3 (430–0 cm depth, ~4000 cal a BP–Present)

4.3.3.1. Pollen. Two subzones can be differentiated on the basis of proportional changes between *Nothofagus* and Poaceae pollen. While *Nothofagus* percentage increases upcore from 62 to 73% in subzone LF-3a (~4000–~1100 cal a BP), expressing the dominance of a closed forest, Poaceae maintains frequencies similar to the previous subzone (12%). Low pollen values (<9%) are recorded for *Empetrum*/Ericaceae, Asteraceae subf. Asteroideae and Cyperaceae, while *Misodendrum* values increase up to 4.5% relative to the previous subzone (LF-2b). Total pollen concentrations rise to 12,000 grains/g due to increase in *Nothofagus* pollen. Subzone LF-3b (~1100–0 cal a BP) shows an upcore decline in *Nothofagus* from 77 to 60%, accompanied by increases in *Misodendrum* (7%). Poaceae steadily increases upcore (19%) along with Cyperaceae (13%) and Chenopodiaceae (2%). The highest total pollen concentration values are registered in this subzone, with 22,800 grains/g at 54 cm depth.

4.3.3.2. Algae. Subzone LF-3a displays an increase in *Pediastrum kawraiskyi* values (24%) while *Botryococcus braunii* shows a marked decline (15–26%) relative to the previous subzone. During subzone LF-3b, *B. braunii* frequencies increase abruptly (41–66%), along with decreases in *P. kawraiskyi* (14–21%). At the top of this subzone (LF-3b), *B. braunii* declines (18%) to values similar to those of *P. kawraiskyi* (16%).

4.4. Palynofacies analysis

Palynofacies signifies a sediment sequence containing a distinctive assemblage of palynological matter considered to reflect a specific set of environmental conditions. A particular palynofacies may also be associated with a characteristic range of hydrocarbon-generating potential (Tyson, 1995). As previously described by several authors (e.g., Traverse, 1994; Tyson, 1995; Batten, 1996), many variables are involved in the deposition of palynological matter. Integration of lithologic data, palynofacies and organic geochemical data provides valuable information for a more accurate interpretation of depositional environments. According to the cluster analysis performed for this study (Fig. 8), three palynofacies types have been recognized in core LF06-PC16, based on the relative frequencies of the four identified categories of palynological matter (Table 4).

4.4.1. Type 1-palynofacies (P1)

Palynofacies P1 (Fig. 7M and N), found only in one sample (49), is characterized by the predominance of opaque phytoclasts having the highest values (62%) of all the analyzed palynofacies. Blade-shaped types (10 to 40 μm in length) are more abundant than equidimensional ones. While translucent phytoclasts represent nearly 31% of the total palynological matter, the palynomorph and amorphous organic matter groups are scarce (4 and 2%, respectively). The Zooclast group represents only 1% of the total palynological matter in this palynofacies.

4.4.2. Type 2-palynofacies (P2)

Palynofacies P2 (Fig. 7O and P) has been identified in samples 1, 9, 14, 18, 23, 27, 32 and 54 and is characterized by the highest proportion of translucent phytoclasts (64–82%) that are light to medium brown colored, poorly preserved and predominantly non-biostructured. Opaque phytoclasts represent between 7 and 28% of the total palynological matter with predominance of blade-shaped types. The amorphous organic matter group, mainly spongy type, is very scarce (up to 3%). The Palynomorph group amounts do not surpass 8%, except in samples 9 and 14 (up to 17%). The Zooclast group ranges between 0 and 2.5% (in average 1%).

4.4.3. Type 3-palynofacies (P3)

This palynofacies (Fig. 7Q and R) occurs in samples 3, 5, 7, 37, 42 and 60 and shows higher phytoclast proportion than in the previous palynofacies (P2); however, translucent phytoclasts vary from 42 to 54%, with a predominance of biostructured types (yellow to light brown fungal hyphae). Opaque phytoclasts, mainly blade-shaped fragments, exhibit higher percentage values than in the previous palynofacies (P2) (17–39%, with a mean of 31%). Amorphous organic matter group, mainly spongy type, is very scarce (up to 2.5%), except in sample 7, where it makes up 11%. The Palynomorph group exhibits the highest proportion of all the samples (11–18%, with mean percentage of 14%). The Zooclast group is more abundant than in the previous palynofacies (P2), varying from 0 to 5% (3% in average).

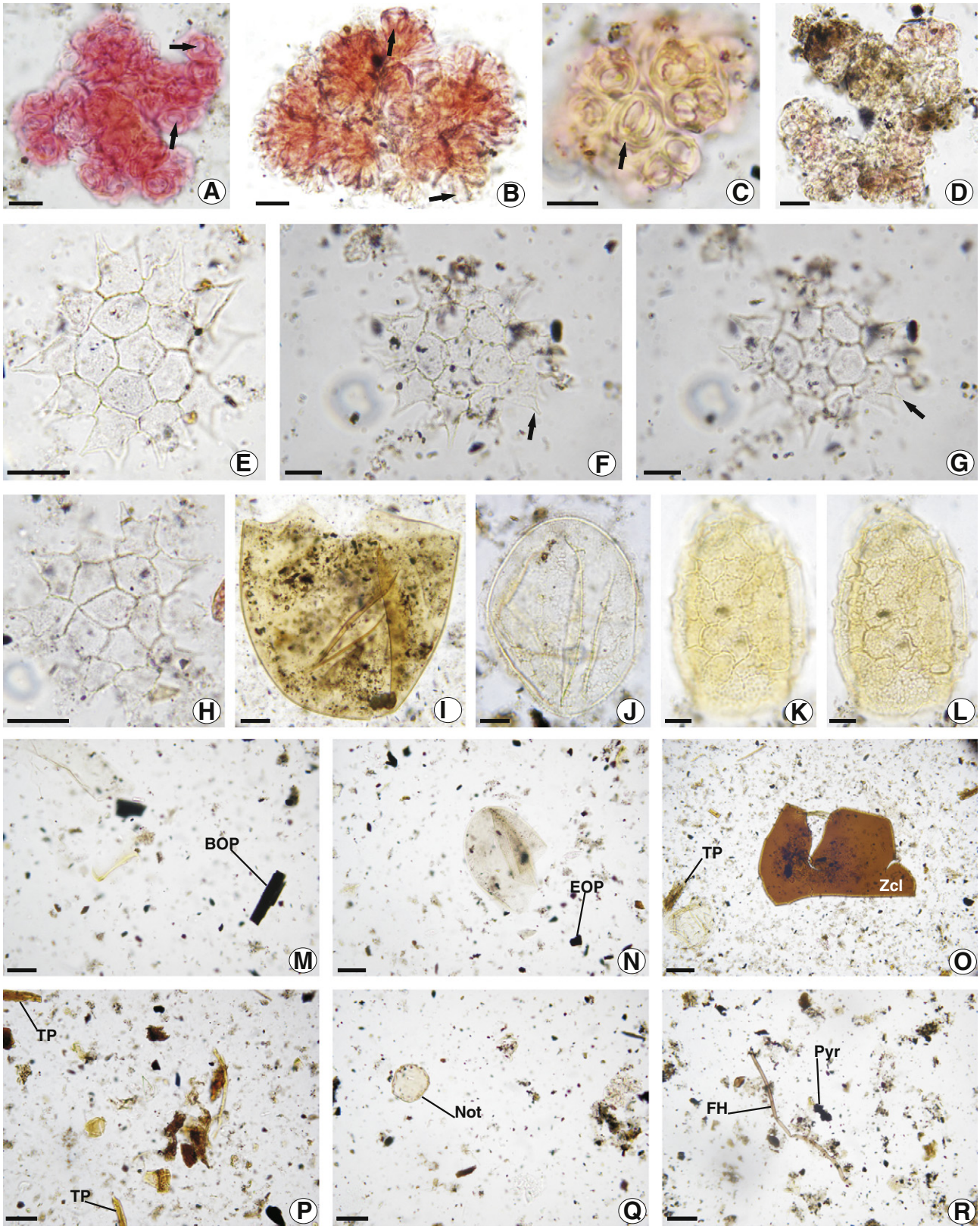

Fig. 7. Algae, non-pollen palynomorphs and palynofacies types from the LF06-PC16 core. A–C) Well-preserved colonies of *Botryococcus braunii*. A) Sample 3: J42/3, branched compound colony showing detail of the cavities cups without autospores in surface view. B) Sample 3: H14/1, compound botryoidal colony showing pear-shaped cavities cups radially arranged. C) Sample 7: C36/4, compound botryoidal colony showing growth rings. D) Sample 3: N25/3, highly-degraded branched compound colony of *Botryococcus braunii* showing patches of structureless mass. E to H) Well-preserved coenobia of *Pediastrum kawraiskyi*. E) Sample 3: M23/1. F and G) Sample 3: Q49/3, two focuses of the same specimen showing the characteristic lobes of the external cells oriented in different planes. H) Sample 3: J47/3. I) Neorhabdocoela oocyte, Sample 37: N55/3. J) Rotifer egg, sample 9: P30/4. K and L) Rotifer egg, sample 9: Q29/4. M and N) Palynofacies P1, sample 49, BOP: blade-shaped opaque phytoclast, EOP: equidimensional opaque phytoclast. O and P) Palynofacies P2, samples 23 and 14, respectively. Zcl: zooclast, TP: translucent phytoclast. Q and R) Palynofacies P3, sample 5. Not: *Nothofagus dombeyi* type, FH: fungal hyphae, Pyr, disseminated pyrite. Scale bar = 10 μm, except M, N, P, Q, and R = 25 μm and O = 50 μm.

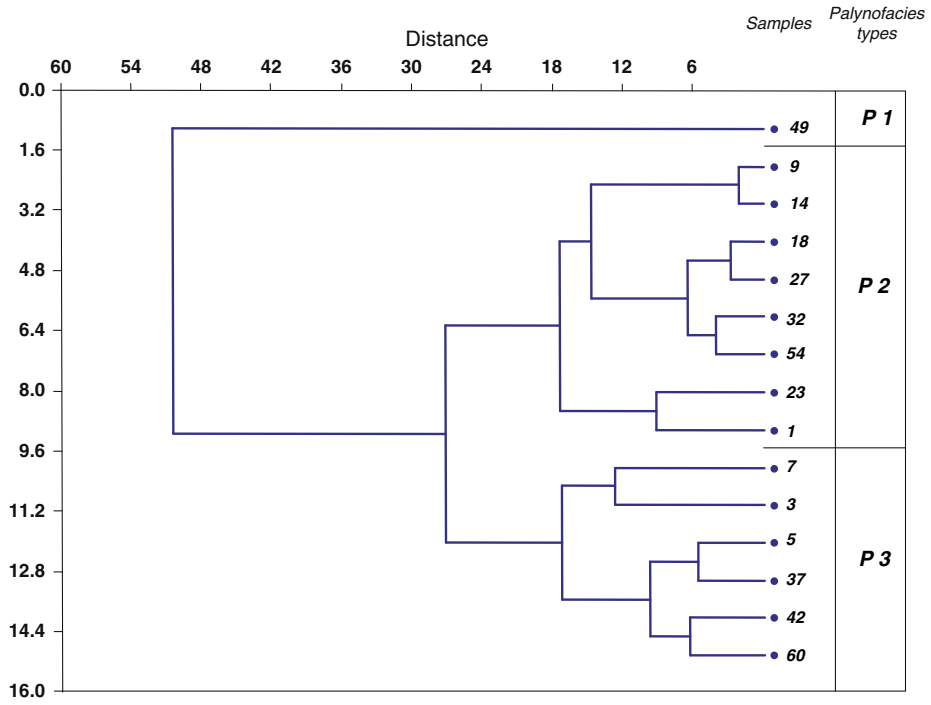

Fig. 8. Cluster analysis and types of palynofacies from core LF06-PC16. Three principal palynofacies are recognized in this core, P1–P3 (see text for more details).

4.5. Diatoms

4.5.1. Modern diatom flora

Selected samples from a N–S transect in the western basin (LF06-G5 to LF06-G13; see Fig. 1D for location) were used to identify modern diatom assemblages. Taxonomical and quantitative analyses show a highly diverse diatom community, with species from the genus *Discostella* (Houk and Klee, 2004) being visibly dominant (Fig. 9). *Discostella stelligera* and *Discostella mascarenica* (Klee et al., 2000) represent more than 80% of the diatoms found in the sediment. Amongst the minoritary taxa, the most abundant are the Fragilariaceae species, particularly *Staurosirella pinnata* and others such as *Fragilaria capucina*, *Pseudostaurosira brevistriata*, *Synedrella parasitica* and *Distrionella germainii*. The benthos and epiphyton are highly dominated by various Achnanthoid species such as *Karayevia clevei* and *Planothidium lanceolatum* as well as the genera *Enyonema* (e.g., *E. elginense*) and *Cymbella* (e.g., *C. cistula*). *Cocconeis* is also well represented with *Cocconeis neothumensis* and *Cocconeis placentula* var. *euglypta*. Concentration of planktonic diatoms becomes higher at the deeper areas of the lake, as it is expected in such a water column, especially the centric *Discostella mascarenica*. The near shore areas contain 80% of planktonic species and 20% of non-planktonic (benthic and epiphytic), varying towards the center of the lake to 91 and 9% planktonic and non-planktonic taxa, respectively.

4.5.2. Fossil diatom assemblages

Diatom assemblages in the FA05-3 core are characterized by high variability with over a hundred identified species, yet clearly one species dominates: *Discostella stelligera*. Diatom concentration (expressed in number of valves/mg dry sediment) shows a relatively uniform trend with values fluctuating between 600,000 and 1,320,000 valves/mg (Fig. 10).

Due to the overall dominance of *Discostella stelligera* (mean: 80–90%), its concentration is not considered in the total percentage calculation displayed in the diagram; the relative abundances of all the other species are calculated omitting *D. stelligera* from the record. Therefore, these values represent relative variations within the minoritary taxa. The planktonic species *Discostella mascarenica* decreases from bottom to top in the lowermost half of the core whereas an opposite trend is observed for the non-planktonic species, particularly the most abundant genus, the benthic *Encyonema*. Other benthic taxa like *Karayevia clevei*, *Cymbella* spp., *Staurosirella pinnata*, *Fragilaria* spp., *Synedra* spp., *Achnanthes* spp., *Navicula* spp., and epiphytic taxa like *Cocconeis placentula* and *Gomphonema* spp. exhibit similar trends. An opposite trend characterizes an intermediate zone up to the top 20 cm, where the ratio between plankton and non-plankton decreases again towards present times.

Table 4
Frequencies (%) of the palynologic matter (PM) types extracted from LF06-PC16 core. There are four main PM groups (see text for more details).

Sample	Phytoclast group		Amorphous group	Palynomorph group	Zooclast group
	Translucent	Opaque			
P 1	75.83	13.36	3.15	7.66	0
P 3	54.2	25.2	2	15.2	3.4
P 5	42.5	39.4	1.3	13.8	3
P 7	50.5	17.5	11	18	3
P 9	68	12.5	0	17.3	2.2
P 14	68	13	1	15.5	2.5
P 18	68	20	2	8	1.5
P 23	82.4	6.93	2.37	8.3	0
P 27	67	21.6	3	6.2	2.2
P 32	63.6	27.75	1.35	7.32	0
P 37	44.6	34.8	1	16.4	3.2
P 42	49	34	0.8	11.7	4.5
P 49	30.95	62.13	1.78	4.14	1
P 54	66.4	24.75	1.6	7.05	0.2
P 60	53	33	2.5	11.5	0

5. Interpretation

5.1. Sedimentology and chronology

The cyclic alternation of brown clay and black organic-enriched laminae that typifies core FA05-3 and most of core LF06-PC16, lithological units W4 and E1, respectively, suggest sedimentation in a well-

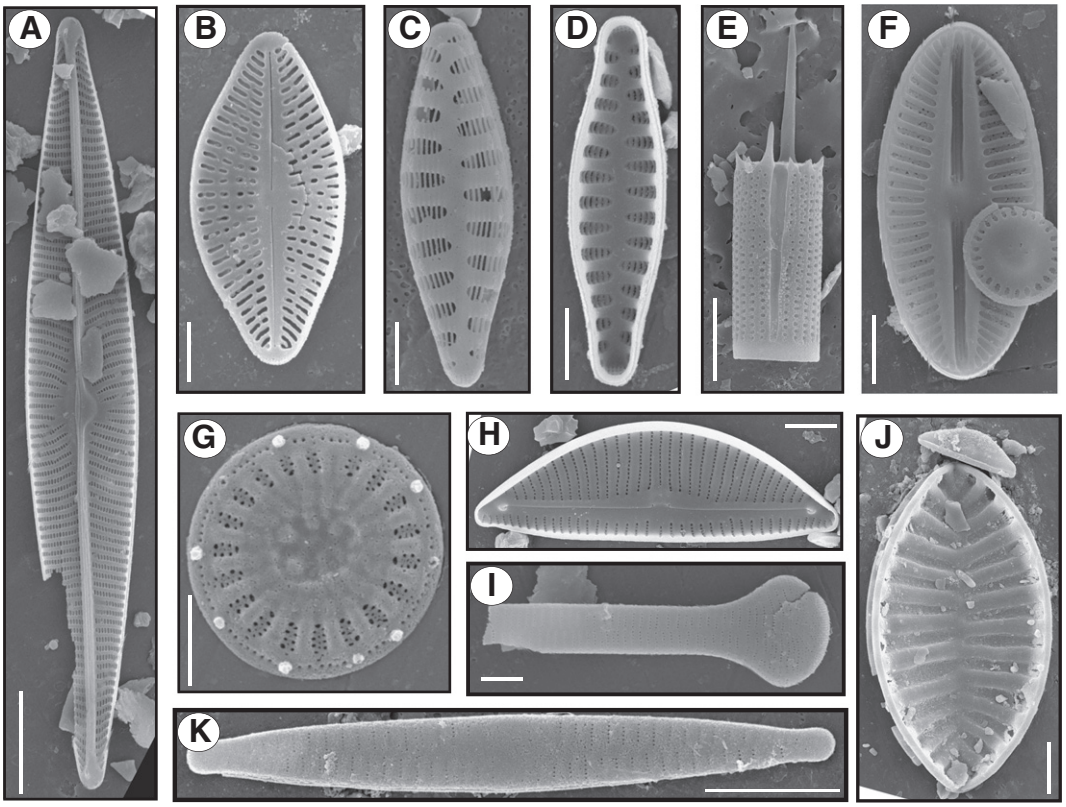

Fig. 9. SEM micrographs of some of the dominant modern and fossil diatom species from surface samples at various water depths in Lago Fagnano and from the LF-05-3 gravity core. A) *Navicula radiosa*. B) *Karayevia clevei*. C–D) External and internal view of *Staurosirella pinnata*. E) *Aulacoseira granulata*. F) *Diploneis chilensis*. G) *Discostella mascarenica*. H) *Encyonema* spp. I) *Fragilaria germainii*. J) *Surirella* spp. K) *Fragilaria capucina*. Scale bar = 2 μm, except A, E = 10 μm and F, K = 5 μm.

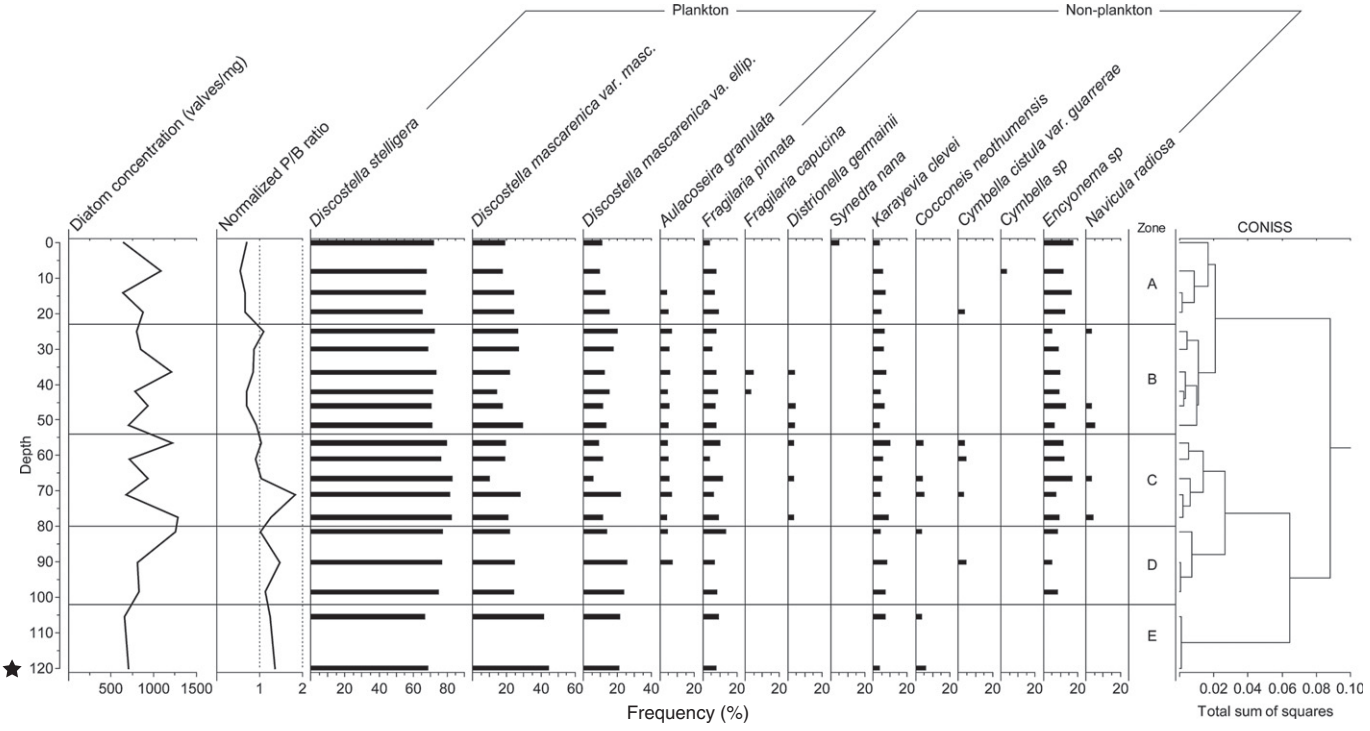

Fig. 10. Diatom diagram for gravity core FA05-3, showing diatom concentration (in million valves per gram dry sediment) and relative abundances between the dominant taxa (relative abundance >3% in at least one sample). Given that *Discostella stelligera* dominates the record, the other species abundances have been recalculated to 100% for the plot. Diatom biozones and the cluster analysis are also shown in the figure.

stratified lake yielding high organic matter content. This stratification may have induced anoxic or dysoxic conditions in the sediment/water interface, thereby explaining the absence of bioturbation and the sporadic presence of vivianite in both cores (Postma, 1981; Lamoureux and Gilbert, 2004).

The tephra layer recovered in both cores and dated to ~7500 cal a BP (Waldmann et al., 2010a) separates the sampled sedimentary sequence into a younger section, characterized by high organic content, and an older, more organic-depleted sequence. Fe content in Lago Fagnano sediments has been interpreted to represent an indirect proxy of paleoprecipitation (Waldmann et al., 2010a). The temporal trend in both the inorganic and organic content of the lake sediments indicates increasing nutrient supply, and thus an evolution from a lake with low productivity to one with high nutrient content. The latter is associated with both algal blooms and the predominance of hypoxic conditions at the lake floor.

Based on the radiocarbon dates obtained from core LF06-PC16 and the robust identification of the H1 tephra in both cores, we are able to estimate an age for the recovered sedimentary sequences in the two sub-basins suggesting that the sedimentary unit cored in the eastern sub-basin reach 11,300 cal a BP, while that of the western sub-basin represented in core LF05-3 spans 7500 cal a BP. The different sedimentation rates observed in the two sub-basins are probably the result of frequent turbidites occurring in the eastern sub-basin, while they are almost entirely absent in the western sub-basin (Waldmann et al., 2011). Moreover, the main input of clastic and detrital material to the lake occurs in the easternmost sub-basin, thus promoting a westwards decrease in sedimentation rate (Waldmann et al., 2010a).

5.2. Palynological and organic matter analyses

5.2.1. Palynomorphs

The basal section of core LF06-PC16 (zone LF-1, ~11,300– ~ 8000 cal a BP) is characterized by pollen-starved samples (insufficient for the analysis). At 6.61 m depth (~10,140 cal a BP), the only one sample with pollen abundance shows non-arboreal taxa mainly characterized by Poaceae (grasses), in association with *Empetrum* (dwarf shrub heaths), Asteraceae subf. Asteroideae (scrubs), Cyperaceae (sedges) and Polypodiaceae (ferns). Also, the freshwater algae-starved samples suggest that water conditions in the lake hampered growing conditions for these algae probably as a consequence of alkaline pH, high oxidation potential (Eh) and intense biological activity (Bryant et al., 1994, p. 54). In spite of this, the initial record of both *Botryococcus braunii* and *Pediastrum kawraiskyi* indicate very cold, clean water, oligotrophic or dystrophic conditions (Břízová, 2009) probably due to the freshwater input from glaciers in the watershed (Waldmann et al., 2010b). At 6.61 m depth, the upcore high amounts of *Botryococcus braunii* suggest oligotrophic conditions and probably low lake levels. Similar studies of Quaternary lake sediments from Africa, Western Australia and sub-Andean Colombia have shown that *Botryococcus*, characteristic of oligotrophic waters, is abundant and associated with low lake levels or littoral zones from large lakes, saline conditions and drier periods (Tyson, 1995; Mensing et al., 2004). Yet, this statement needs to be strengthened and better confirmed for high-latitude lacustrine settings such as Lago Fagnano.

Considering caveats related to the lower amount of samples in subzone LF-2a, the *Nothofagus* forest is recorded along with grasses, shrubs and heaths from ~8000 to 7000 cal a BP. These plant assemblages correspond to an open landscape characterized by the forest-steppe ecotone. This vegetation assemblage, which today includes patches of *Nothofagus antarctica* forest, occurs in areas of central Tierra del Fuego with annual precipitation estimated at 400–500 mm and summer temperatures averaging 10–11 °C (Heusser, 2003). The record of both *Botryococcus braunii* and *Pediastrum kawraiskyi* algae indicate persistent oligotrophic conditions and the presence of *Pediastrum kawraiskyi* suggest cooler water conditions than in the previous zone (LF-1). This species represents a cold stenotherm, typifying a boreal environment of clear and pure oligo- or mesotrophic waters with pH higher than 7, probably connected with peat areas in the coastal zones (Komárek and Jankovská, 2001; Zamaloa and Tell, 2005). Significant occurrences of halophyte vegetation (Chenopodiaceae) characterize those areas close to the margins of the lake, as the increased record of Neorhabdocoela oocytes (Fig. 7I) may stand for lower lake stands and higher water temperatures (Haas, 1996).

After ~6000 cal a BP (subzone LF-2b), the *Nothofagus* forest shows an open structure, allowing the existence of light-demanding species, such as herbs (Poaceae) and ferns (Polypodiaceae). These plant assemblages resemble the *Nothofagus pumilio* woodland near the steppe, suggesting that the mean annual precipitation must have increased to at least 500 mm (Pendall et al., 2001). The oligotrophic conditions appear to have been maintained during this subzone. However, the abundance of *Pediastrum kawraiskyi* declines, along with higher values of Neorhabdocoela oocytes, indicating that the lake waters were probably slightly warmer compared to previous conditions in subzone LF-2a.

The recorded high *Nothofagus* pollen frequency and concentrations between ~4000 and 1100 cal a BP imply the presence of a closed forest around the lake during subzone LF-3a, pointing to higher effective moisture levels. The record of grasses and sedges (Cyperaceae) may indicate vegetal communities growing along the margins of the lake (Moore, 1983). Today, the development of a dense *Nothofagus* forest occurs in the south of Tierra del Fuego, where the mean annual precipitation ranges from 500 to 800 mm/yr and mean annual temperatures average 6.5 °C (Pisano, 1977; Heusser, 1998). The rise in *Pediastrum kawraiskyi* frequencies, in coincidence with a closed *Nothofagus* forest, might imply an increasing meteoric water input under colder conditions and higher effective moisture, thus resulting in a decrease of *Botryococcus braunii* frequencies. Moreover, rotifers occur in lakes with pH higher than 7 and feed on detritus (van Geel et al., 2000), so that their resting eggs are related to seasonal rainfall (Limaye et al., 2007). The increased record of rotifer resting eggs in subzone LF-3a (Fig. 7J to L) might therefore indicate increased runoff during this interval.

After ~1100 cal a BP (subzone LF-3b), the decline in *Nothofagus* frequencies and the increasing amounts of grass (Poaceae), sedge (Cyperaceae) and fern (Polypodiaceae) taxa suggest an open forest environment with development of grasses and sedges. The lake maintained its oligotrophic state, while increasing values of *Botryococcus braunii* suggest lower lake levels than during the previous subzone (LF-3a).

5.2.2. Palynofacies

The high opaque phytoclast frequencies (62%) in palynofacies P1 (sample 49, Table 3) indicate long-distance or long-duration of transport from sources of phytoclasts and oxidizing environments (Tyson, 1995). The blade/equant frequency of black phytoclast particles can be used in palynofacies studies to indicate proximal–distal variations (Martínez et al., 2008). Thus, the high values of blade/equant reinforce the interpretation of distal settings.

In palynofacies P2 (Fig. 8), the high percentages of translucent phytoclasts (~73%) may indicate two different paleoenvironmental interpretations (Tyson, 1995): i) high terrestrial organic matter contributions as a result of dilution of other components (e.g., lake autochthonous organic matter), implying proximity to a fluvial source with high TOC values (as observed in samples 1, 9, 14, 18, 23 and 27; Table 3); or ii) low organic content values, suggesting oxidizing environments in which other components have been selectively destroyed (samples 54 and 32, Table 3). The latter situation is reinforced in sample 54 by the predominance of degraded and darker phytoclasts (Table 3).

The predominance of translucent phytoclasts (48% in average), accompanied by the highest frequencies of the palynomorph group (as observed mainly in samples 3, 5 and 7, Table 3) in palynofacies P3 (samples 3, 5, 7, 37, 42 and 60, Table 3) suggest close proximity to fluvial sources. In samples 37, 42 and 60, the slight increase in opaque phytoclasts (averaging 31%) indicate moderate oxidant environments.

This palynofacies (P3, Fig. 8) comprises most of the samples with the highest *Botryococcus braunii* frequencies, suggesting enhanced evaporation and salinity of lake waters under drier conditions. Development of halophyte vegetation (Chenopodiaceae) as recorded in our palynological record, is common from saline soils on the banks of ponds, temporary pools and edges of brackish water lakes (Břízová, 2009).

5.3. Diatom analysis

Modern diatom assemblages are typical of an oligotrophic lake. The diatom flora recorded in core FA05-3 is relatively homogeneous throughout the studied time interval suggesting relatively stable environmental conditions. Analyzing the minoritary diatom taxa reveals as well relatively homogenous assemblages in both the current surface sediments and those retrieved from the core record. The most dominant species, *Discostella stelligera* and *Dicostella mascarenica*, are both planktonic and point to an oligotrophic lake (De Wolf, 1982; Urrutia et al., 2000). The benthic taxa identified throughout the entire record are most probably transported from the shore areas, considering that the core is located at a water depth of 120 m where no light penetration prevails. The transport of non-planktonic taxa from the shallower areas could be an indicator of strong waves and related water turbulence, probably in relation with intense wind activity. The presence of epiphytic species (*Cocconeis*, *Epithemia*, and *Gomphonema*) in the core may thus serve to indicate the presence of macrophytes growing in the shallower areas that were subsequently brought to the deeper regions by wind-induced water turbulence. This situation will probably enhance transport of epiphytic diatoms attached to macrophytes to the deeper regions. Moreover, the SHW is strengthened in the Fagnano region during spring and summertime (Waldmann et al., 2008), bringing more nutrients into the lake system and triggering an increase in algal blooms, including diatoms.

6. Paleoenvironmental reconstruction

Cores LF06-PC16 and FA05-3 served as the key archives for paleoenvironmental reconstruction presented in this study. Their chronology was well-constrained and framed with the H1 tephra layer and several robust radiocarbon ages. Despite to possible uncertainties due to the pollen and diatom sampling interval and caveats related to the radiocarbon dating, the combination of the retrieved results with data from previous studies (e.g., Moy et al., 2009; Waldmann et al., 2010a; Fig. 10B and C) have improved our capabilities to correctly reconstruct the paleoenvironmental conditions of the region. This exercise has enabled us to further compare our records with other regional proxies in order to assess the spatial impact of millennial-scale climate change on the environment and biota of Tierra del Fuego and to understand the influence of the SHW to the region throughout the entire Holocene.

6.1. Early Holocene (11.5–8.0 cal yr BP)

Paleoclimate reconstructions from southern Patagonia (50–53°S) (McCulloch and Davies, 2001; Whitlock et al., 2007; Moreno et al., 2010) and Tierra del Fuego (Heusser, 2003; Markgraf and Huber, 2010) show increasing temperatures and fire frequencies for the early Holocene along with highly variable precipitation regimes (Fig. 11D). In the Lago Fagnano record, the pollen-barren nature of the recovered sediments may represent alkaline conditions within the lake, following the last stages of deglaciation of the Fagnano glacier (Waldmann et al., 2010b). The only sample with pollen abundance at ~10,140 cal a BP (Fig. 11A) shows grass steppe vegetation. Moreover, the palynofacies analysis suggests the presence of mainly oxidizing environments, with moderate to high transport of palynological matter from distant sources. According to the algal record, a cool and oligo-mesotrophic lacustrine environment developed in the lake, probably resulting from increased input of glacial melt-water. Concurrently, a forest-steppe ecotone developed along the Beagle Channel (Heusser, 1998; Borromei and Quattrocchio, 2008; Markgraf and Huber, 2010), evidencing the prevalence of low humidity conditions, while further north at ~41°S, the podocarp flora index reflects seasonally dry climate (Moreno et al., 2010; Fig. 11E). The reconstruction of humid conditions in Tierra del Fuego based on our multi-proxy study closely follows the annual precipitation pattern at 50°S reconstructed from fossil pollen data (Tonello et al., 2009; Fig. 11F). The paleo-vegetation assemblages as inferred from most of the pollen records during the early Holocene in southern Patagonia imply lower precipitation compared to present conditions, probably related to moisture-laden conditions and weakening SHW.

6.2. Middle Holocene (8.0–3.0 cal yr BP)

The pollen records from southwestern Patagonia (50°S) (Villa-Martinez and Moreno, 2007; Tonello et al., 2009) indicate a trend of increasing precipitation during the mid-Holocene (Fig. 11F). In Tierra del Fuego, along the Beagle Channel area, the *Nothofagus* woodland vegetation and the high fire activity lasted up to ~7000 cal a BP after which a more dense *Nothofagus* forest started to spread (Markgraf and Huber, 2010). Meanwhile, the forest-steppe ecotone evolved in the Lago Fagnano area by ~8000 cal a BP under lower moisture availability, as is reflected by the pollen records from Fagnano mire (Heusser, 2003) and in the pollen samples from our record (Zone LF2, Fig. 11A). By this time, the palynofacies analysis suggests in the lake moderate oxic environments. The algal content, aquatic microfossils and halophyte vegetation indicate oligotrophic conditions paired with enhanced evaporation and salinity under moderate water temperatures.

Carbon isotope values ($\delta^{13}C$) occurring between ~7000 and ~5000 cal a BP in Lago Fagnano, show organic debris enriched in ^{13}C, probably representing increased summer temperatures and enhanced phytoplankton productivity in the lake (Moy et al., 2011). The highest values in $\delta^{13}C$ during this time interval are in coincidence with low C/N values (Moy et al., 2011; Fig. 11C), further suggesting that the mid-Holocene $\delta^{13}C$ peak is indeed related to enhanced aquatic productivity.

Co-variability of our palynological dataset with the $\delta^{13}C$ and C/N record from Lago Fagnano, probably represent evidence for an increase of runoff erosion in the watershed due to higher local precipitation. The increase in moisture availability is also evidenced by the development of a dense *Nothofagus* forest around Lago Fagnano (Heusser, 2003), Lago Yehuin (Markgraf, 1993), Estancia Río Claro (Burry et al., 2006), and also by the migration of the forest-steppe ecotone to the northwest of the Fagnano lake at the Onamonte site after ~5800 cal a BP (Heusser, 1993). Since moisture mainly arrives from the Pacific Ocean carried by the SHW, intensification of the regional wind activity during the mid-Holocene is likely linked to an increase in rain frequency, as identified in other archives as well (Tonello et al., 2009; Fig. 11F).

6.3. Late Holocene (3.0–0.0 cal yr BP)

An increase in precipitation between 50° and 55°S occurred in the late Holocene and has been associated with an intensification of the SHW and the onset of Neoglacial advances in southernmost Patagonia (Moreno et al., 2010; Waldmann et al., 2010a; Moy et al., 2011; Schimpf et al., 2011, and references therein). Prominent increases in precipitation levels were reported from the Andean region between 50° and 53°S (Tonello et al., 2009; Moreno et al., 2010; Fig. 11F). Also, a similar climate pattern has been recorded along the Beagle Channel (Heusser, 1998) and in the Isla de los Estados (Unkel et al., 2008; Ponce et al., 2011; Björck et al., 2012) at 4500 and 4000 cal a BP, respectively. In the latter site, the presence of *Drymis winteri* confirms the development of a Subantarctic Evergreen Forest indicative of highly humid and cold conditions (Ponce et al., 2011). By this time, the

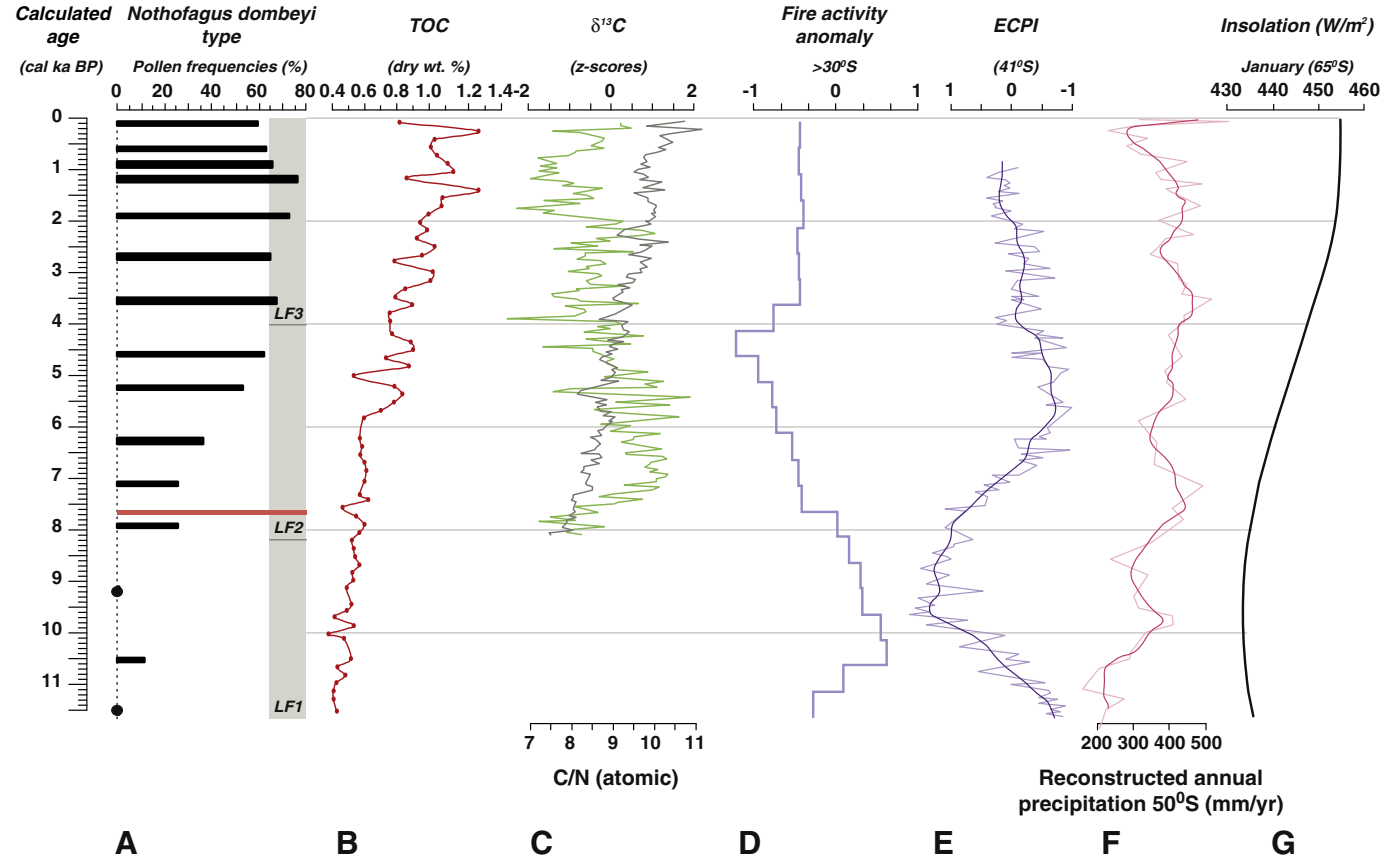

Fig. 11. Comparison of Lago Fagnano data with other regional paleoclimatological proxies. The timing of the Hudson H1 tephra is marked by a red dashed line. A) Frequencies (%) of the *Nothofagus dombeyi* type pollen in Lago Fagnano with the respective palynlogical zones marked by gray bars. B) Total organic concentration (TOC) in Lago Fagnano sediments (Waldmann et al., 2010a). C) $\delta^{13}C$ profile (green) and C/N variability (blue) obtained from Lago Fagnano (Moy et al., 2011). D) Fire activity anomaly in Patagonia south of 30°S (Moreno et al., 2010). E) Lago Condorito record (41°S) of Eucryphia + Caldcluvia/podocarp index (ECPI) (Moreno et al., 2010). F) Reconstructed annual precipitation (mm/yr) at ~50°S, based on a pollen-climate calibration model (Tonello et al., 2009). G) January insolation curve for 65°S (Berger and Loutre, 1991).

forest-steppe ecotone expanded further to the northeast of Tierra del Fuego, at the Cabo San Pablo site (Heusser and Rabassa, 1995) while forest communities are recorded in the area of Lago Fagnano (Heusser, 2003). Moreover, the increase in *Pediastrum kawraiskyi* algae after ~5000 cal a BP and the high record of rotifer resting eggs suggest cool conditions in the lake, probably as a result of increased runoff. During this time interval, the dominancy of planktonic diatom species indicates the establishment of long-term oligotrophic conditions in the lake. Yet, the presence of non-planktonic photosynthetic diatoms probably point to the amplification of SHW winds throughout this time interval.

The relatively low sampling resolution of the pollen and diatom records prevent determination of the extent and magnitude of the Medieval Climate Anomaly (MCA) and the Little Ice Age (LIA) events as was previously recognized in other regional archives (Kastner et al., 2010; Ponce et al., 2011; Schimpf et al., 2011; Dowdeswell and Vásquez, 2013, among others). However, these climatic events have been reported in Lago Fagnano by fluctuations in Fe content (Waldmann et al., 2010a), and were mentioned as well in multi-proxy analyses of peat-bogs in inland areas (Mauquoy et al., 2004; Borromei et al., 2010). Furthermore, the LIA event is consistent with previously reported glacier advances in Tierra del Fuego (Planas et al., 2002; Coronato et al., 2005). Therefore, increasing the sampling interval in the Fagnano sediments would likely provide valuable information about the impact of these climatic intervals on the environmental conditions in the region.

7. Final remarks

The following points summarize the main outcome of this study:

a) This study confirms that sediments from Lago Fagnano provide a unique and important tool for ecological and environmental reconstructions in Tierra del Fuego throughout the Holocene. This multi-proxy study serves as a base for future high-resolution paleoclimate studies in the region.
b) The freshwater algae *Botryococcus braunii* and *Pediastrum kawraiskyi* recorded in the sedimentary archive of Lago Fagnano are for the first time identified in Holocene lacustrine deposits in the Fuegian Archipelago. Their fluctuations are considered to be associated with hydrological changes and nutrient status and may indicate oscillations in lake-level.
c) This study presents the first record of diatom flora from Lago Fagnano. Our study shows that diatom assemblages in this lake are very stable and seem to be poorly affected by Holocene environmental changes, while the terrestrial paleo-vegetation is very sensitive to those climatic changes.
d) Changes in the terrestrial paleo-vegetation communities are related to temporal changes in the wind intensity and latitudinal position of the SHW belt throughout the Holocene.
e) The recovery of a complete sedimentary archive sensitive to paleoclimate changes in the inner part of Tierra del Fuego is crucial to accomplish an effective and comprehensive study of regional

paleoenvironmental changes in the southernmost extreme of South America.

Acknowledgments

We acknowledge Robert Dunbar (Stanford University, USA) for the invaluable help and contributions to every aspect of this study and for the use of the capable small research vessel, the *R/V Neecho* (owned by Stanford). John H. McAndrews (Toronto University, Canada) and Charles L. Turton (Royal Ontario Museum, Canada) are gratefully acknowledged for their valuable help in non-pollen palynomorph identifications. The authors kindly acknowledge Rosanna Martini and Agathe Martignier from the University of Geneva and André Piuz from the Muséum d'Histoire Naturelle de Genève (Switzerland) for their help with SEM imaging. We thank David Mucciarone (Stanford, USA), Steffen Saustrup and Mark Wiederspahn (Institute for Geophysics) and Juan Federico Ponce (CADIC-CONICET) for technical assistance during fieldwork and at later stages of this project. The logistical help, hospitality and assistance during every aspect of the fieldwork of Alejandro, Maria Elena and Gabriel Echeverría from Bahía Torito are also kindly acknowledged. Captains Jorge Ebling and Rafael Quezada are also kindly acknowledged for their help during fieldwork. The Centro Austral de Investigaciones Científicas-Consejo Nacional de Investigaciones Científicas y Técnicas (CADIC-CONICET, Argentina) and the Prefectura Naval Argentina are acknowledged for their logistical support and assistance. This work is part of the project Environmental Changes Down-South (ENDS), supported by the Swiss National Science Foundation grants 200021-100668/1 and 200020-111928/1 to D. Ariztegui and the National Geographic Society (grant CRE 7705-04) to J. A. Austin Jr. We also thank the Augustin Lombard Foundation for their financial support (grant to C. Recasens) for the 2006 field campaign.

References

Auer, V., 1960. The quaternary history of Fuego–Patagonia. Proc. R. Soc. Lond. Ser. B Biol. Sci. 152 (949), 507–516.
Battarbee, R.W., 1984. Diatom analysis and the acidification of lakes. Philos. Trans. R. Soc. Lond. B Biol. Sci. 305 (1124), 451–477.
Battarbee, R.W., 1986. Diatom analysis. Handbook of Holocene Palaeoecology and Palaeohydrology 527–570.
Batten, D.J., 1996. Colonial Chlorococcales. In: Jansonius, J., McGregor, D.C. (Eds.), Palynology: Principles and Applications. American Association of Stratigraphic Palynologists Foundation, pp. 191–203.
Berger, A., Loutre, M.F., 1991. Insolation values for the climate of the last 10000000 years. Quat. Sci. Rev. 10 (4), 297–317.
Bertrand, S., Araneda, A., Vargas, P., Jana, P., Fagel, N., Urrutia, R., 2012. Using the N/C ratio to correct bulk radiocarbon ages from lake sediments: insights from Chilean Patagonia. Quat. Geochronol. 12, 23–29.
Björck, S., Rundgren, M., Ljung, K., Unkel, I., Wallin, Å., 2012. Multi-proxy analyses of a peat bog on Isla de los Estados, easternmost Tierra del Fuego: a unique record of the variable Southern Hemisphere Westerlies since the last deglaciation. Quat. Sci. Rev. 42, 1–14.
Borromei, A.M., 1995. Pollen analysis from a Holocenic peat in the Valley of Andorra, Tierra de Fuego, Argentina. Rev. Chil. Hist. Nat. 68 (3), 311–319.
Borromei, A., Quattrocchio, M., 2008. Late and postglacial paleoenvironments of Tierra del Fuego terrestrial and marine palynological evidence. In: Rabassa, J. (Ed.), Late Cenozoic of Patagonia and Tierra del Fuego. Elsevier, pp. 369–382.
Borromei, A.M., Coronato, A., Franzén, L.G., Ponce, J.F., Sáez, J.A.L., Maidana, N., Rabassa, J., Candel, M.S., 2007a. Multiproxy record of Holocene paleoenvironmental change, Tierra del Fuego, Argentina. Palaeogeogr. Palaeoclimatol. Palaeoecol. 206, 1–6.
Borromei, A.M., Coronato, A., Quattrocchio, M., Rabassa, J., Grill, S., Roig, C., 2007b. Late Pleistocene–Holocene environments in Valle Carbajal, Tierra del Fuego, Argentina. J. S. Am. Earth Sci. 23 (4), 321–335.
Borromei, A., Coronato, A., Franzen, L.G., Ponce, F., López Sáez, J.A., Maidana, N., Rabassa, J., Candel, M.S., 2010. Multiproxy record of Holocene paleoenvironmental change, Tierra del Fuego, Argentina. Palaeogeogr. Palaeoclimatol. Palaeoecol. 286, 1–6.
Břízová, E., 2009. Quaternary environmental history of the Čejčské Lake (S. Moravia, Czeche Republic). Bull. Geosci. 84 (4), 637–652.
Bryant Jr., V.M., Holloway, R.G., Jones, J.G., Carlson, D.L., 1994. Pollen preservation in alkaline soils of the American Southwest. In: Traverse, A. (Ed.), Sedimentation of Organic Particles. Cambridge University Press, pp. 47–58.
Burry, L.S., de Mandri, M.T., DAntoni, H.L., 2006. Paleocomunidades vegetales del centro de Tierra del Fuego durante el Holoceno temprano y tardío. Rev. Mus. Argent. Cienc. Nat. 8 (2), 127–133.
Candel, M.S., Borromei, A.M., Martínez, M.A., Gordillo, S., Quattrocchio, M., Rabassa, J., 2009. Middle–Late Holocene palynology and marine mollusks from Archipiélago Cormoranes area, Beagle Channel, southern Tierra del Fuego, Argentina. Palaeogeogr. Palaeoclimatol. Palaeoecol. 273 (1–2), 111–122.
Coronato, A., Seppälä, M., Rabassa, J., 2005. Last Glaciation landforms in Lake Fagnano ice lobe, Tierra del Fuego, Southernmost Argentina. 6th International Conference on Geomorphology, Zaragoza, Spain.
Coronato, A., Seppälä, M., Ponce, J.F., Rabassa, J., 2009. Glacial geomorphology of the Pleistocene Lake Fagnano ice lobe, Tierra del Fuego, southern South America. Geomorphology 112 (1–2), 67–81.
De Wolf, H., 1982. Method of coding of ecological data from diatoms for computer utilization. Med. Rijks Geol. Dienst. Nieuwe Ser. 36 (2), 95–110.
Dowdeswell, J.A., Vásquez, M., 2013. Submarine landforms in the fjords of southern Chile: implications for glacimarine processes and sedimentation in a mild glacier-influenced environment. Quat. Sci. Rev. 64, 1–19.
Faegri, K., Iversen, J., 1989. Textbook of Pollen Analysis. Copenhagen.
Farr, T.G., Rosen, P.A., Caro, E., Crippen, R., Duren, R., Hensley, S., Kobrick, M., Paller, M., Rodriguez, E., Roth, L., Seal, D., Shaffer, S., Shimada, J., Umland, J., Werner, M., Oskin, M., Burbank, D., Alsdorf, D., 2007. The shuttle radar topography mission. Rev. Geophys. 45 (2), RG2004.
Garreaud, R.D., Vuille, M., Compagnucci, R., Marengo, J., 2009. Present-day South American climate. Palaeogeogr. Palaeoclimatol. Palaeoecol. 281 (3), 180–195.
Grill, S., Borromei, A.M., Quattrocchio, M., Coronato, A., Bujalesky, G., Rabassa, J., 2002. Palynological and sedimentological analysis of recent sediments from Río Varela, Beagle Channel, Tierra del Fuego, Argentina. Rev. Esp. Micropaleontol. 34 (2), 145–161.
Grimm, E.C., 1987. CONISS: a FORTRAN 77 program for stratigraphically constrained cluster analysis by the method of incremental sum of squares. Comput. Geosci. 13, 13–35.
Grimm, E.C., 1993. TILIA v2.0 (computer software). Illinois State Museum, Research and Collections Center, Springfield.
Grimm, E.C., 2004. "Tilia graph v. 2.0. 2." Illinois state museum, research and collections center.
Haas, J.N., 1996. Neorhabdocoela oocytes—palaeoecological indicators found in pollen preparations from Holocene freshwater lake sediments. Rev. Palaeobot. Palynol. 91 (1), 371–382.
Hammer, Ø., Harper, D.A.T., Ryan, P.D., 2001. PAST: paleontological statistics software package for education and data analysis. Palaeontol. Electron. 4 (1), 9.
Heusser, C.J., 1989. Late Quaternary vegetation and climate of southern Tierra del Fuego. Quat. Res. 31, 396–406.
Heusser, C.J., 1993. Late Quaternary forest-steppe contact zone, Isla Grande de Tierra del Fuego, Subantarctic South America. Quat. Sci. Rev. 12, 169–177.
Heusser, C.J., 1998. Deglacial paleoclimate of the American sector of the Southern Ocean: Late Glacial–Holocene records from the latitude of Canal Beagle (55°S), Argentine Tierra del Fuego. Palaeogeogr. Palaeoclimatol. Palaeoecol. 141 (3–4), 277–301.
Heusser, C.J., 2003. Ice Age Southern Andes: a chronicle of paleoecological events. Developments in Quaternary Sciences Elsevier Science Ltd. 240.
Heusser, C.J., Rabassa, J., 1987. Cold climatic episode of Younger Dryas age in Tierra del Fuego. Nature 328, 609–611.
Heusser, C., Rabassa, J., 1995. Late Holocene forest–steppe interaction at Cabo San Pablo, Isla Grande de Tierra del Fuego, Argentina. Quat. S. Am. Antarct. Penins. 9, 179–188.
Houk, V., Klee, R., 2004. The stelligeroid taxa of the genus Cyclotella (Kutzing) Brebisson (Bacillariophyceae) and their transfer into the new genus Discostella gen. nov. Diatom Res. 19 (2), 203–228.
Juggins, S., 2003. C2 user guide. Software for Ecological and Palaeoecological Data Analysis and VisualizationUniversity of Newcastle, Newcastle Upon Tyne, UK (69 pp.).
Kalnay, E., Kanamitsu, M., Kistler, R., Collins, W., Deaven, D., Gandin, L., Iredell, M., Saha, S., White, G., Woollen, J., Zhu, Y., Chelliah, M., Ebisuzaki, W., Higgins, W., Janowiak, J., Mo, K.C., Ropelewski, C., Wang, J., Leetmaa, A., Reynolds, R., Jenne, R., Joseph, D., 1996. The NCEP/NCAR 40-year reanalysis project. Bull. Am. Meteorol. Soc. 77 (3), 437–471.
Kastner, S., Enters, D., Ohlendorf, C., Haberzettl, T., Kuhn, G., Lücke, A., Mayr, C., Reyss, J.L., Wastegård, S., Zolitschka, B., 2010. Reconstructing 2000 years of hydrological variation derived from laminated proglacial sediments of Lago del Desierto at the eastern margin of the South Patagonian Ice Field, Argentina. Glob. Planet. Chang. 72 (3), 201–214.
Klee, R., Houk, V., Bielsa, S., 2000. Cyclotella mascarenica nov. Spec., a new stelligeroid Cyclotella (Bacyllariophyceae) from a pond of the Réunion Island (France). Arch. Hydrobiol. 133, 7–25 (Alg. Studies 98).
Komárek, J., Jankovská, V., 2001. Review of the green algal genus Pediastrum: implication for pollen-analytical research. Bibliotheca PhycologicaJ. Cramer, Berlin 127.
Lamoureux, S.F., Gilbert, R., 2004. Physical and chemical properties and proxies of high latitude lake sediments. Long-term Environmental Change in Arctic and Antarctic Lakes 53–87.
Lamy, F., Ruhlemann, C., Hebbeln, D., Wefer, G., 2002. High- and low-latitude climate control on the position of the southern Peru–Chile Current during the Holocene. Paleoceanography 17 (2), 16.1–16.10.
Limaye, R.B., Kumaran, K.P.N., Nair, K.M., Padmalal, D., 2007. Non-pollen palynomorphs as potential palaeoenvironmental indicators in the Late Quaternary sediments of the west coast of India. Curr. Sci. 92 (10), 1370–1382.
Mariazzi, A., Conzzono, V., Ulibarrena, J., Paggi, J., Donadelli, J., 1987. Limnological investigation in Tierra del Fuego, Argentina. Biol. Acuatica 10, 1–74.
Markgraf, V., 1980. Pollen dispersal in a mountain area. Grana 19 (2), 127–146.
Markgraf, V., 1993. Paleoenvironments and Paleoclimates in Tierra-Del-Fuego and Southernmost Patagonia, South-America. Palaeogeogr. Palaeoclimatol. Palaeoecol. 102 (1–2), 53–68.
Markgraf, V., Huber, U.M., 2010. Late and postglacial vegetation and fire history in Southern Patagonia and Tierra del Fuego. Palaeogeogr. Palaeoclimatol. Palaeoecol. 297 (2), 351–366.

Martínez, M.A., Ferrer, N.C., Asensio, M.A., 2008. Primer registro de algas dulceacuícolas del Paleógeno de la Cuenca de Ñirihuau, Argentina: descripciones sistemáticas y análisis palinofacial. Ameghiniana 45 (4), 719–735.
Mauquoy, D., Blaauw, M., van Geel, B., Borromei, A., Quattrocchio, M., Chambers, F.M., Possnert, G., 2004. Late Holocene climatic changes in Tierra del Fuego based on multiproxy analyses of peat deposits. Quat. Res. 61, 148–158.
McCulloch, R.D., Davies, S.J., 2001. Late-glacial and Holocene palaeoenvironmental change in the central Strait of Magellan, southern Patagonia. Palaeogeogr. Palaeoclimatol. Palaeoecol. 173 (3–4), 143–173.
Menichetti, M., Lodolo, E., Tassone, A., 2008. Structural geology of the Fuegian Andes and Magallanes fold-and-thrust belt — Tierra del Fuego Island. Geol. Acta 6 (1), 19–42.
Mensing, S.A., Benson, L.V., Kashgarian, M., Lund, S., 2004. A Holocene pollen record of persistent droughts from Pyramid Lake, Nevada, USA. Quat. Res. 62 (1), 29–38.
Montgomery, D.R., Balco, G., Willett, S.D., 2001. Climate, tectonics, and the morphology of the Andes. Geology 29 (7), 579.
Moore, D.M., 1983. Flora of Tierra del Fuego. Nelson, Oswestry.
Moreno, P.I., François, J.P., Villa-Martínez, R.P., Moy, C.M., 2009. Millennial-scale variability in Southern Hemisphere westerly wind activity over the last 5000 years in SW Patagonia. Quat. Sci. Rev. 28 (1), 25–38.
Moreno, P.I., Francois, J.P., Moy, C.M., Villa-Martinez, R., 2010. Covariability of the Southern Westerlies and atmospheric CO2 during the Holocene. Geology 38 (8), 727–730.
Moy, C.M., Moreno, P.I., Dunbar, R.B., Kaplan, M.R., Francois, J.P., Villalba, R., Haberzettl, T., 2009. Climate change in Southern South America during the last two millennia. Past Climate Variability in South America and Surrounding Regions 14 353–393.
Moy, C.M., Dunbar, R.B., Guilderson, T.P., Waldmann, N., Mucciarone, D.A., Recasens, C., Ariztegui, D., Austin Jr., J.A., Anselmetti, F.S., 2011. A geochemical and sedimentary record of high southern latitude Holocene climate evolution from Lago Fagnano, Tierra del Fuego. Earth Planet. Sci. Lett. 302 (1–2), 1–13.
Musotto, L., Bianchinotti, M.V., Borromei, A.M., 2012. Pollen and fungal remains as environmental indicators in surface sediments of Isla Grande de Tierra del Fuego, southernmost Patagonia. Palynology 36 (2), 162–179.
Naranjo, J.A., Stern, C.R., 1998. Holocene explosive activity of Hudson Volcano, southern Andes. Bull. Volcanol. 59 (4), 291–306.
Pendall, E., Markgraf, V., White, J.W.C., Dreier, M., Kenny, R., 2001. Multiproxy record of Late Pleistocene–Holocene climate and vegetation changes from a peat bog in Patagonia. Quat. Res. 55 (2), 168–178.
Pisano, V.E., 1977. Fitogeografía de Fuego-Patagonia chilena. I. Comunidades vegetales entre las latitudes 52° Y 56° S. An. Inst. Patagonia Punta Arenas, Chile 8, 121–250.
Planas, X., Ponsa, A., Coronato, A., Rabassa, J., 2002. Geomorphological evidence of different glacial stages in the Martial cirque, Fuegian Andes, southernmost South America. Quat. Int. 87 (1), 19–27.
Ponce, J.F., Borromei, A.M., Rabassa, J.O., Martinez, O., 2011. Late quaternary palaeoenvironmental change in western Staaten Island (54.5°S, 64°w), Fuegian Archipelago. Quat. Int. 233, 89–100.
Postma, D., 1981. Formation of siderite and vivianite and the pore-water composition of a recent bog sediment in Denmark. Chem. Geol. 31 (3), 225–244.
Quirós, R., Drago, E., 1999. The environmental state of Argentinean lakes: an overview. Lakes Reserv. Res. Manag. 4 (1), 55–64.
Quirós, R., Baigun, C.R.M., Cuch, S., Delfino, R., de Nichilo, A., Guerrero, C., Marinone, M.C., Menu Marque, S., Scapini, M.C., 1988. Evaluación del rendimiento pesquero potencial de la República Argentina I: Datos 1.
Richter, A., Hormaechea, J.L., Dietrich, D., Perdomo, R., Fritsche, M., Del Cogliano, D., Liebsch, G., Mendoza, L., 2010. Lake-level variations of Lago Fagnano, Tierra del Fuego: observations, modelling and interpretation. J. Limnol. 69 (1), 1–13.
Rogers, J.C., van Loon, H., 1982. Spatial variability of sea level pressure and 500 mb height anomalies over the southern hemisphere. Mon. Weather Rev. 110 (10), 1375–1392.
Schimpf, D., Kilian, R., Kronz, A., Simon, K., Spötl, C., Wörner, G., Deininger, M., Mangini, A., 2011. The significance of chemical, isotopic, and detrital components in three coeval stalagmites from the superhumid southernmost Andes (53°S) as high-resolution palaeo-climate proxies. Quat. Sci. Rev. 30 (3–4), 443–459.
Stern, C.R., 2008. Holocene tephrochronology record of large explosive eruptions in the southernmost Patagonian Andes. Bull. Volcanol. 70 (4), 435–454.
Stockmarr, J., 1971. Tablets with spores used in absolute pollen analysis. Pollen Spores 13, 615–621.
Stuiver, M., Reimer, P.J., Reimer, R.W., 2005. Calib 6.0. http://calib.qub.ac.uk/calib/.
Tonello, M.S., Mancini, M.V., Seppä, H., 2009. Quantitative reconstruction of Holocene precipitation changes in southern Patagonia. Quat. Res. 72, 410–420.
Traverse, A., 1994. Sedimentation of palynomorphs and playnodebris: an introduction. In: Traverse, A. (Ed.), Sedimentation of Organic Particle. Cambridge Press, Cambridge, p. 544.
Tyson, R.V., 1995. Sedimentary Organic Matter. Chapman & Hall, London.
Unkel, I., Björck, S., Wohlfarth, B., 2008. Deglacial environmental changes on Isla de los Estados (54.4°S), southeastern Tierra del Fuego. Quat. Sci. Rev. 27, 1541–1554.
Urrutia, R., Sabbe, K., Cruces, F., Pozo, K., Becerra, J., Araneda, A., Vyverman, W., Parra, O., 2000. Paleolimnological studies of Laguna Chica of San Pedro (VIII Region): diatoms, hydrocarbons and fatty acid records. Rev. Chil. Hist. Nat. 73 (4), 717–728.
van Geel, B., Heusser, C.J., Renssen, H., Schuurmans, C.J.E., 2000. Climatic change in Chile at around 2700 BP and global evidence for solar forcing: a hypothesis. The Holocene 10 (5), 659–664.
Villa-Martinez, R., Moreno, P.I., 2007. Pollen evidence for variations in the southern margin of the westerly winds in SW Patagonia over the last 12,600 years. Quat. Res. 68 (3), 400–409.
Waldmann, N., Ariztegui, D., Anselmetti, F.S., Austin, J.J.A., Dunbar, R., Moy, C.M., Recasens, C., 2008. Seismic stratigraphy of Lago Fagnano sediments (Tierra del Fuego, Argentina) — a potential archive of paleoclimatic change and tectonic activity since the Late Glacial. Geol. Acta 6 (1), 101–110.
Waldmann, N., Ariztegui, D., Anselmetti, F.S., Austin, J.J.A., Moy, C.M., Stern, C., Recasens, C., Dunbar, R., 2010a. Holocene climatic fluctuations and positioning of the Southern Hemisphere Westerlies in Tierra del Fuego (54°S), Patagonia. J. Quat. Sci. 25 (7), 1063–1075.
Waldmann, N., Ariztegui, D., Anselmetti, F.S., Coronato, A., 2010b. Geophysical evidence of multiple glacier advances in Lago Fagnano (54°S), southernmost Patagonia. Quat. Sci. Rev. 29 (9–10), 1188–1200.
Waldmann, N., Anselmetti, F.S., Ariztegui, D., Austin Jr., J.A., Pirouz, M., Moy, C.M., Dunbar, R., 2011. Holocene mass-wasting events in Lago Fagnano, Tierra del Fuego (54°S): implications for paleoseismicity of the Magallanes–Fagnano transform fault. Basin Res. 23, 171–190.
Whitlock, C., Moreno, P.I., Bartlein, P., 2007. Climatic controls of Holocene fire patterns in southern South America. Quat. Res. 68 (1), 28–36.
Zamaloa, M.d.C., Tell, G., 2005. The fossil record of freshwater micro-algae *Pediastrum* Meyen (Chlorophyceae) in southern South America. J. Paleolimnol. 34, 433–444.